Formation and Deposition of Functional Films

Rainer Hippler

University of Greifswald

Koszalin 2008

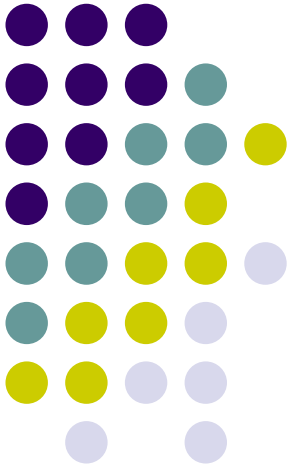

Hansestadt Greifswald

Home town of Caspar David Friedrich

Marktplatz

University of Greifswald

Founded 1456

Physics in Greifswald

2007

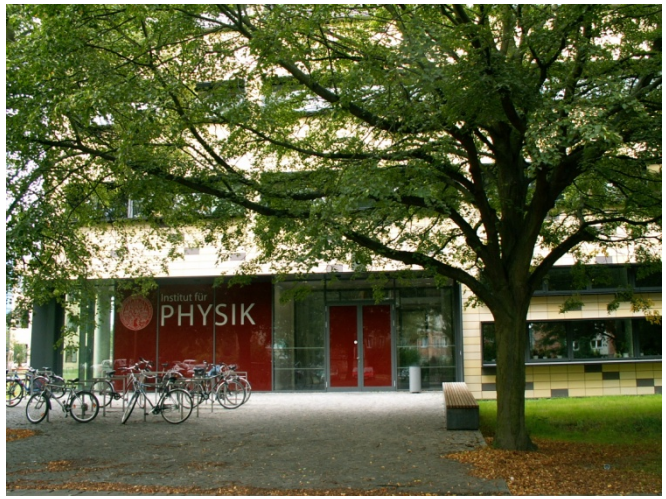

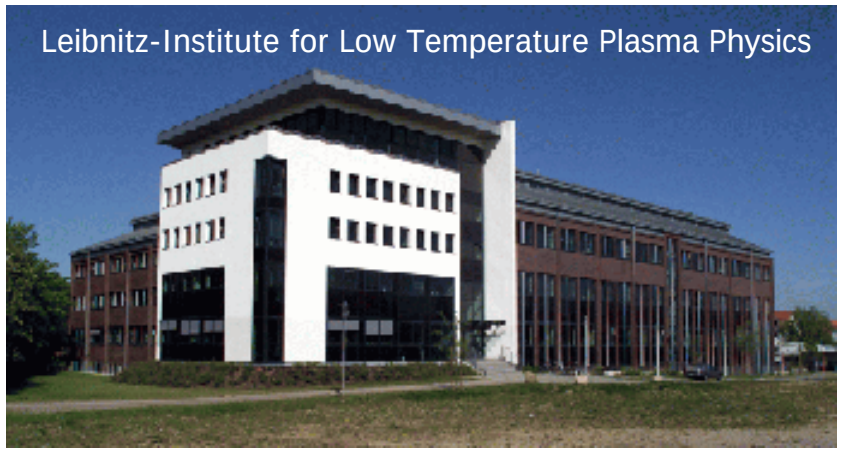

Outline

- Plasma-assisted deposition of thin metal oxide films
- Aplications of functional films
- Nano-size clustern formation and deposition
- Properties of deposited cluster

Plasma-assisted deposition of, e.g., Thin metal oxide films

- Optically transparent
- Electrically conducting
- Large number of potential applications:
  - Glas with low heat conductivity
  - Solar cells
  - Optical coatings
  - Liquid crystal and plasma display panels
  - optoelectronical elements

Plasma-enhanced chemical vapor deposition:

Magnetron discharge

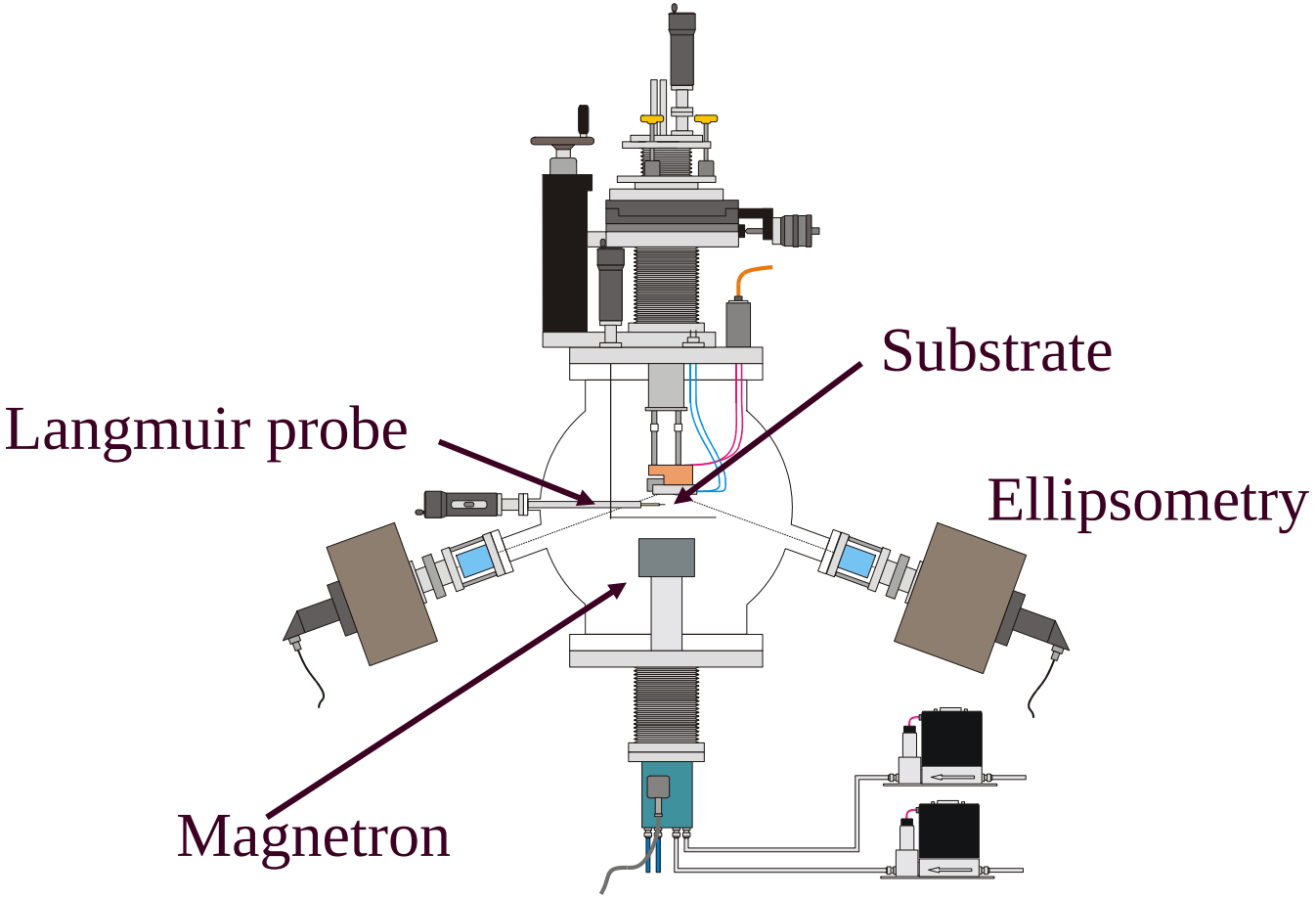

Planar magnetron

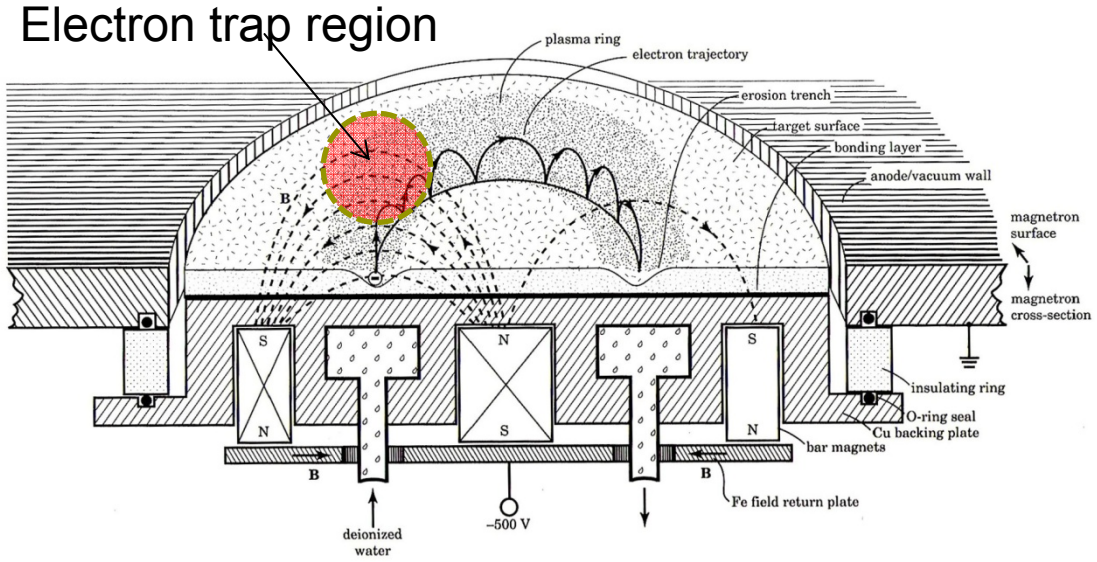

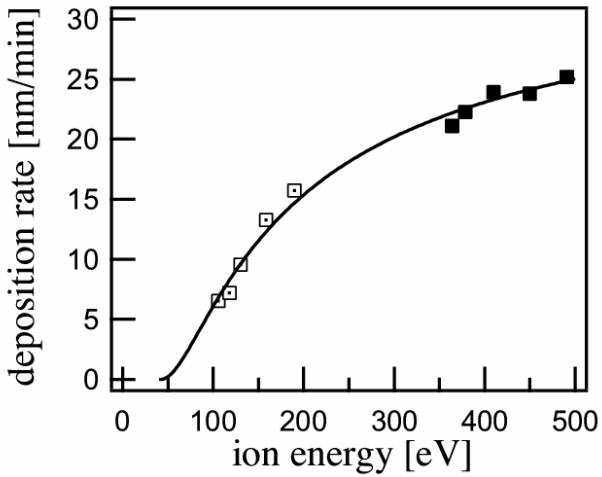

Positve Ions impinging on negatively biased cathode with kinetic energy E ≤ e U produce

- Sputtered target atoms and ions, sputtering yield Y ≈ 0.5
- Secondary electrons, emission coefficient $\gamma \approx 0.05$.
- Secondary electrons gain energy equal to cathode potential and become trapped in the trap region of perpendicular electric and magnetic fields where each energetic electron produces $1/\gamma \approx 20$ ions.

Hall current

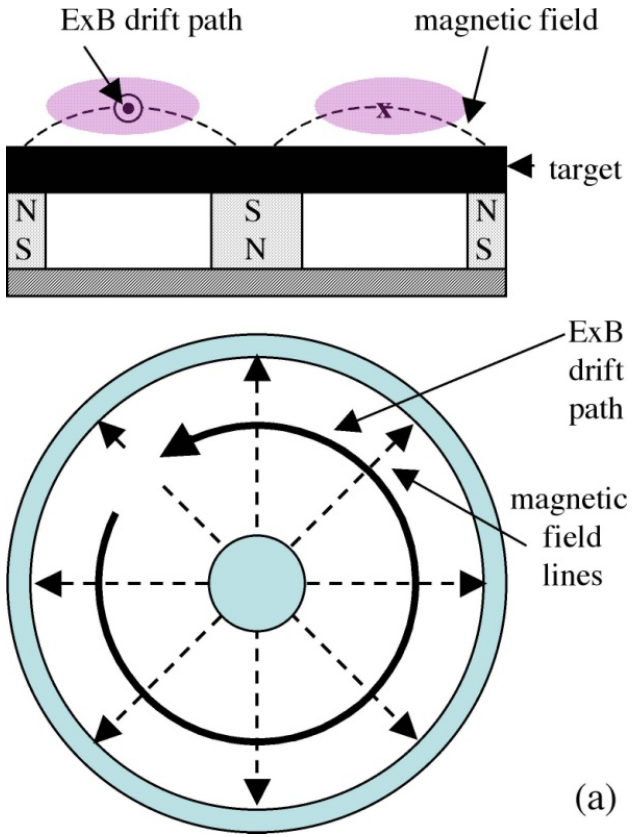

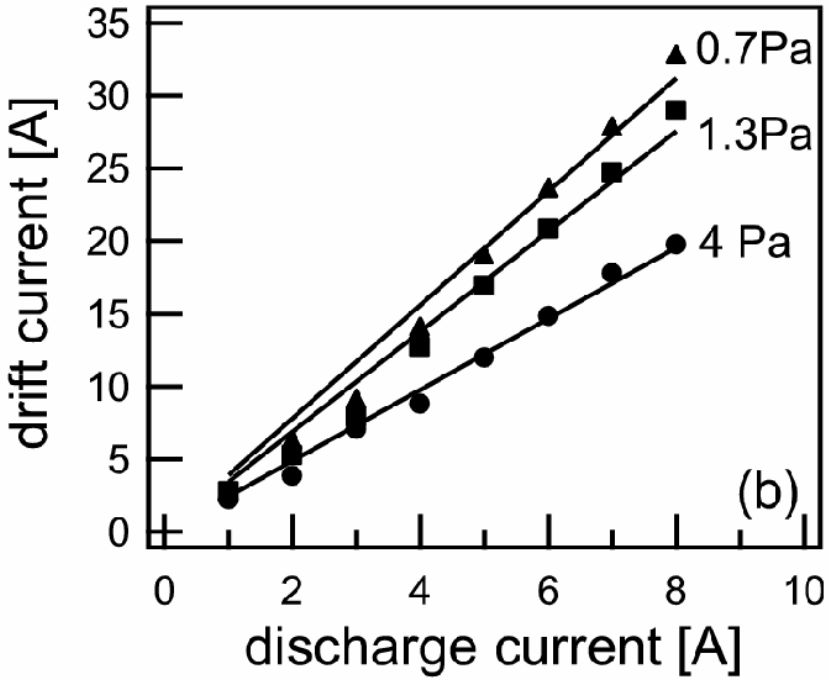

Drift or Hall current can exceed
the discharge current by factors of 3-7.

Magnetron – balanced and unbalanced mode

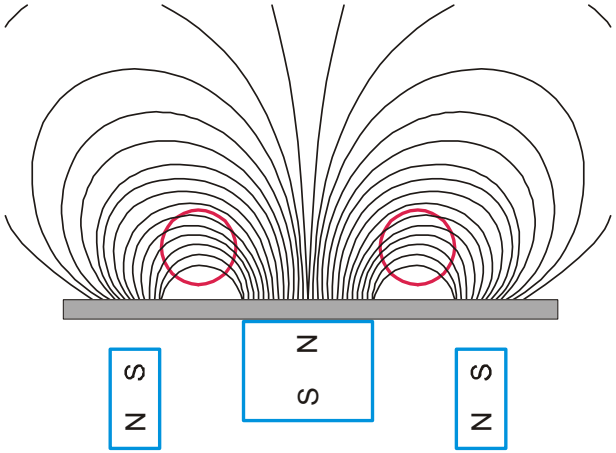

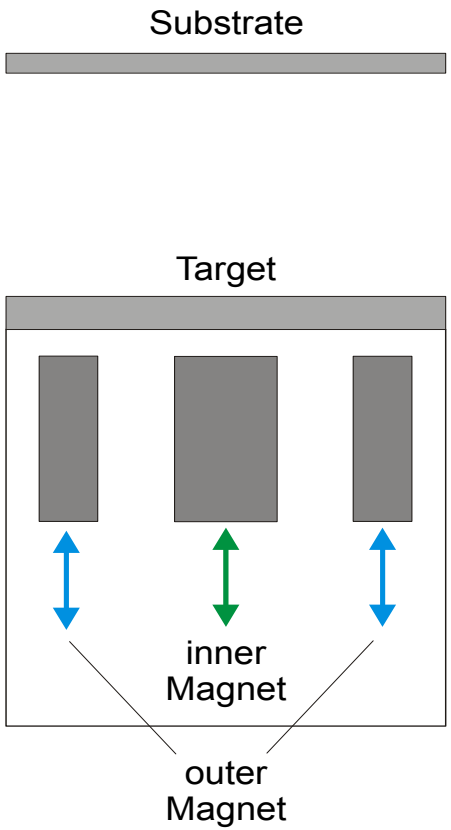

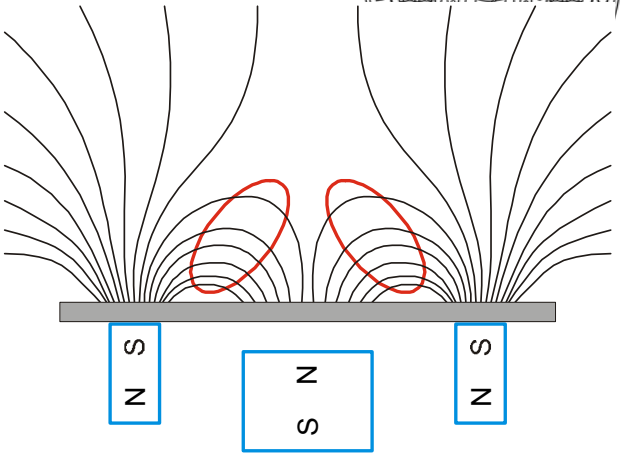

Balanced mode:
inner magnet up -
outer magnet down

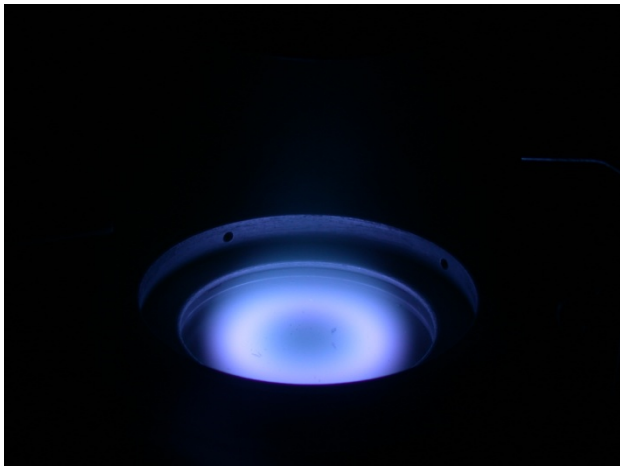

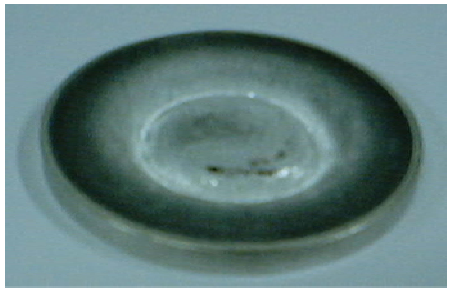

Unbalanced mode:
inner magnet down -
outer magnet up

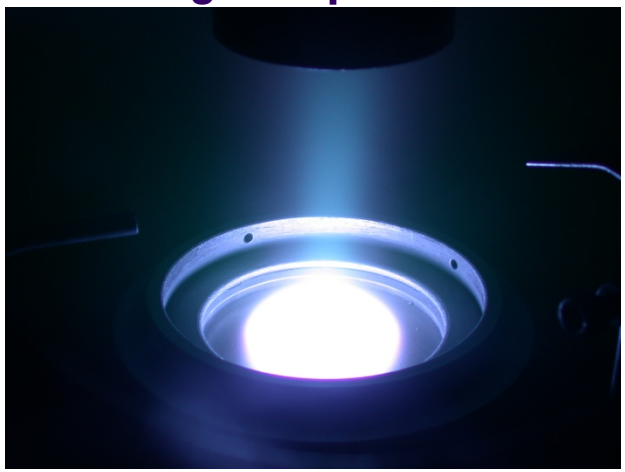

Functional layers:
Glass with low heat conductivity

Heat transport = heat conductivity + Radiation

glass/argon/blocker/glas

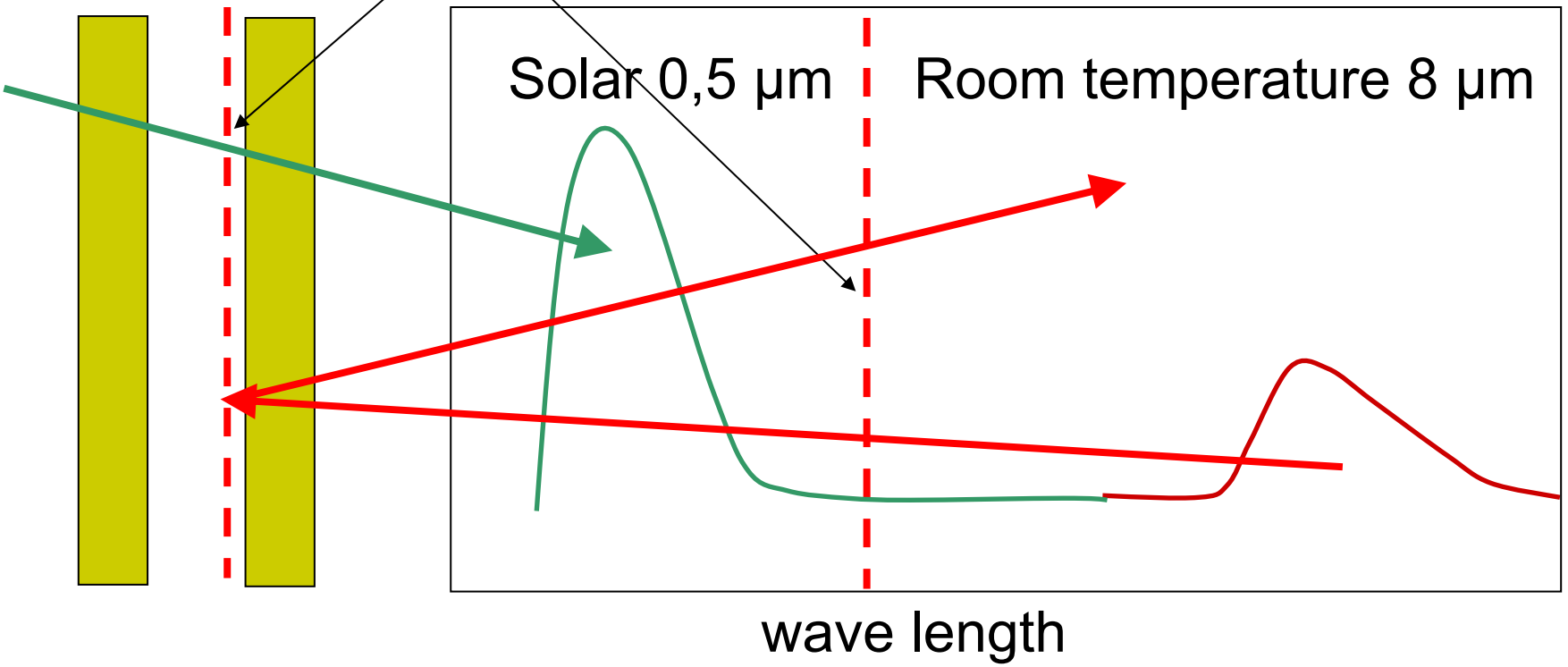

Deposition of Functional layers:
Glass with low heat conductivity
produced by large scale magnetron sputtering

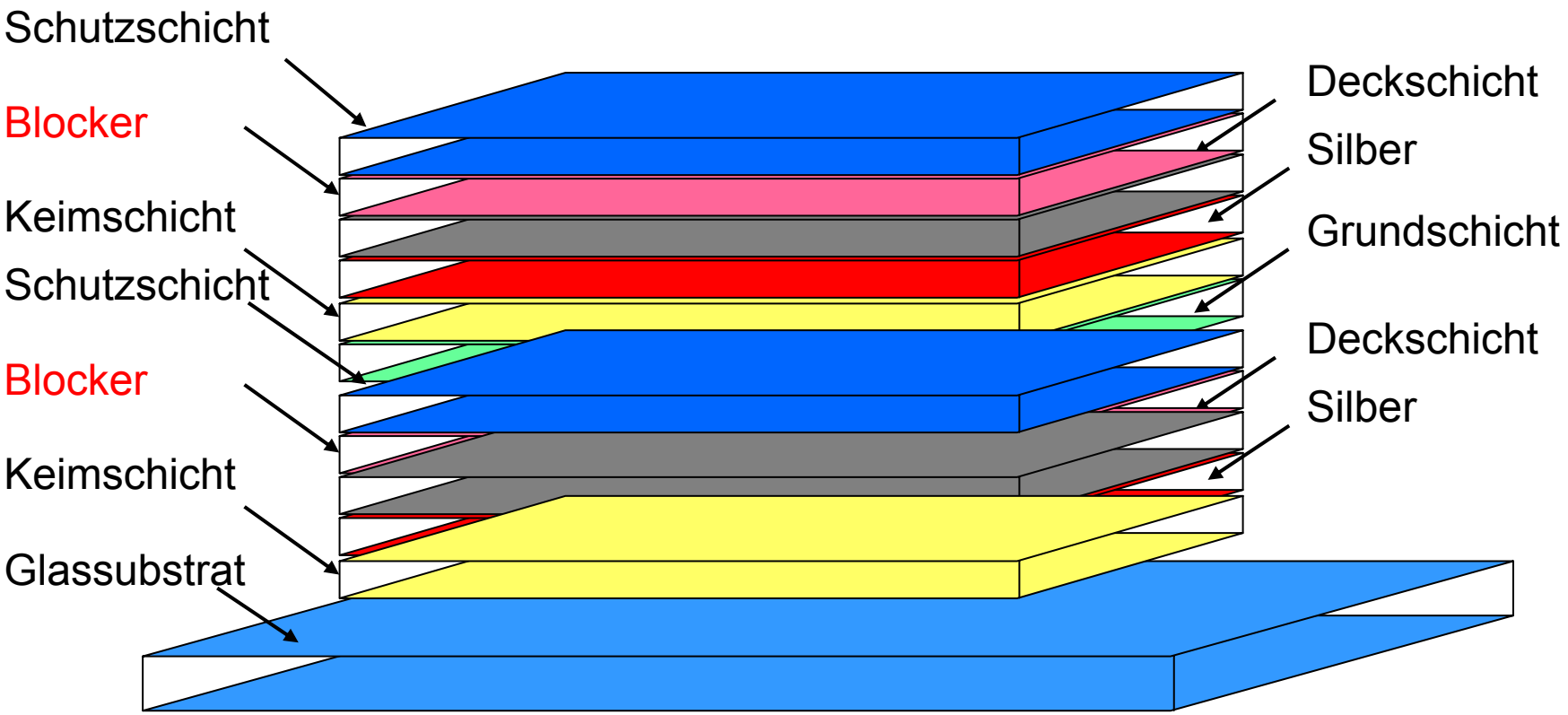

Solar cells

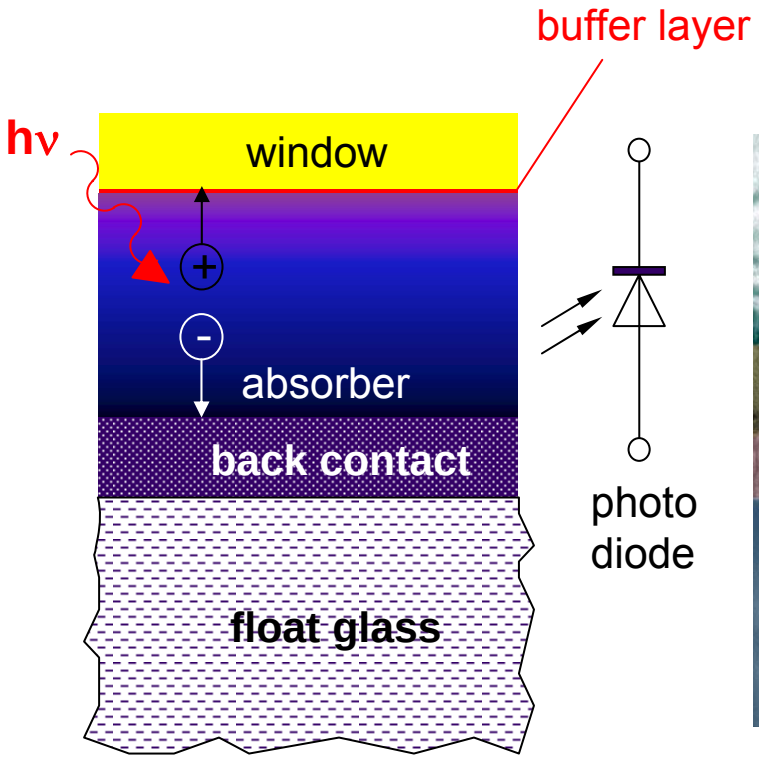

REM cut view

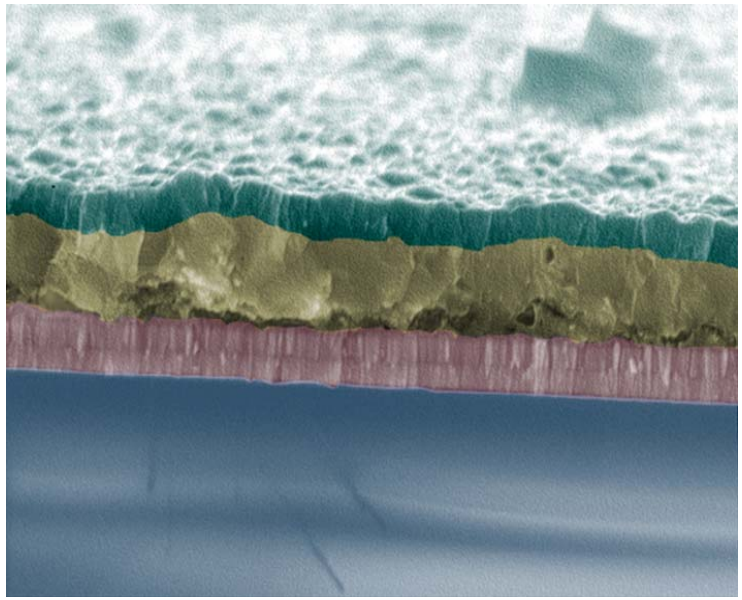

n-ZnO/ZnO:Al
p-$CuInS_2$
Molybdenum

float glass

Photovoltaic materials

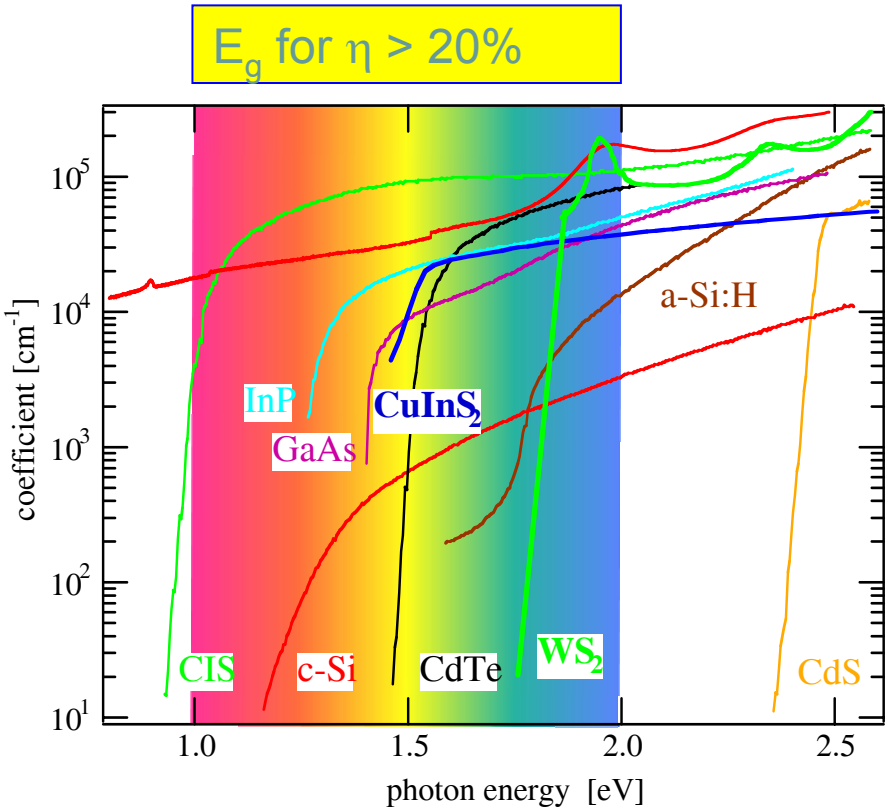

Requirements

- small absoprtion length ($1/\alpha < 0.5$ µm)
- „suitable“ band gap (1-2 eV)
- toxicologically harmless material
- abundunt in Earth crust

Requirements for physical vapour depositions

- Large scale (>> 1 m^2), high deposition rates, cheap
- Low substrate temperatures (< 500 °C).
- Good adhesion, equal films thickness, and high density.
- Depositon of alloys and of composites
- Simple, robust, good long-time stability

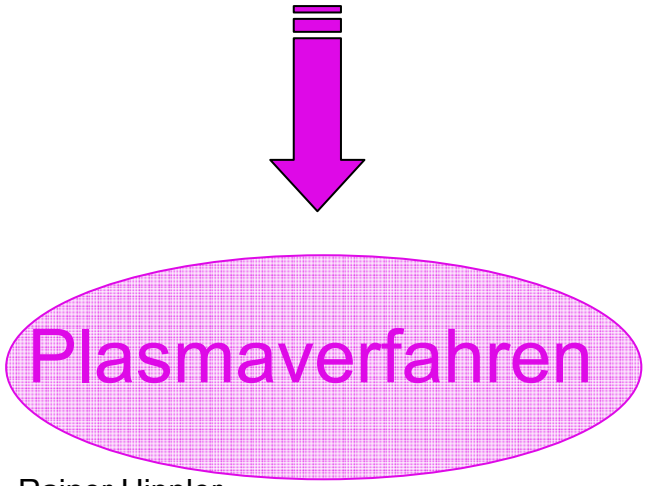

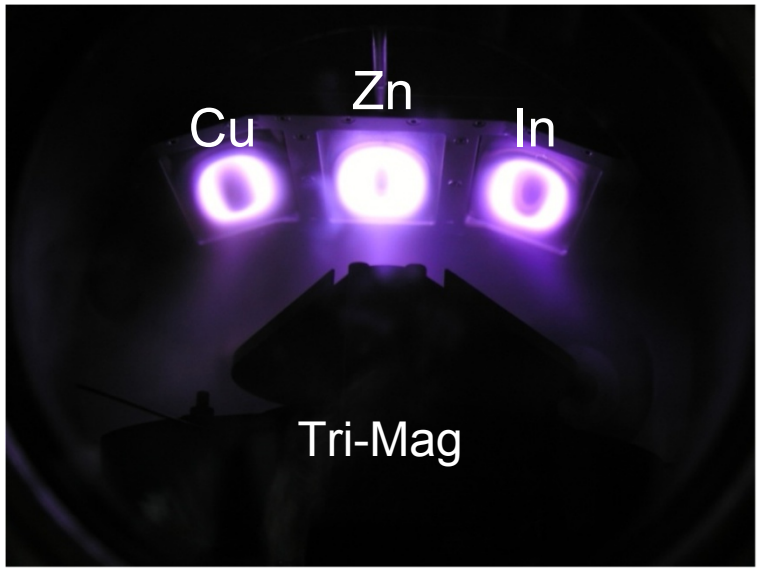

Plasma “films“ in thin film solar cells

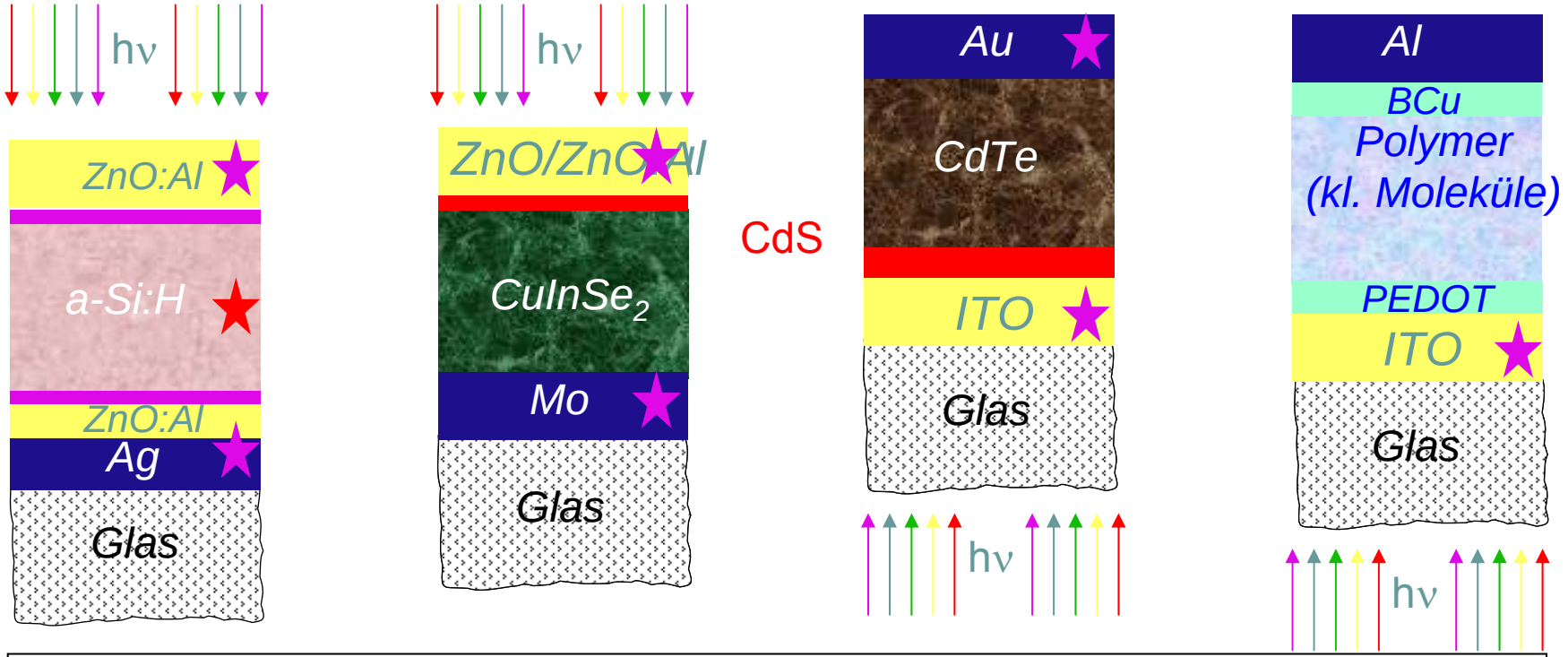

η=12.1%	η =19.9%	η=16.5%	η ≈ 6 %

★ ★ → Deposition employing PECVD or Magnetron sputtering

Plasma diagnostics

- Time-resolved Langmuir probe
- Energy-resolved mass spectroscopy (Plasma process monitor)
- Thermal probe to determine the energy influx
- Optical and tunable diode laser spectroscopy

Plasma diagnostics: Langmuir probe

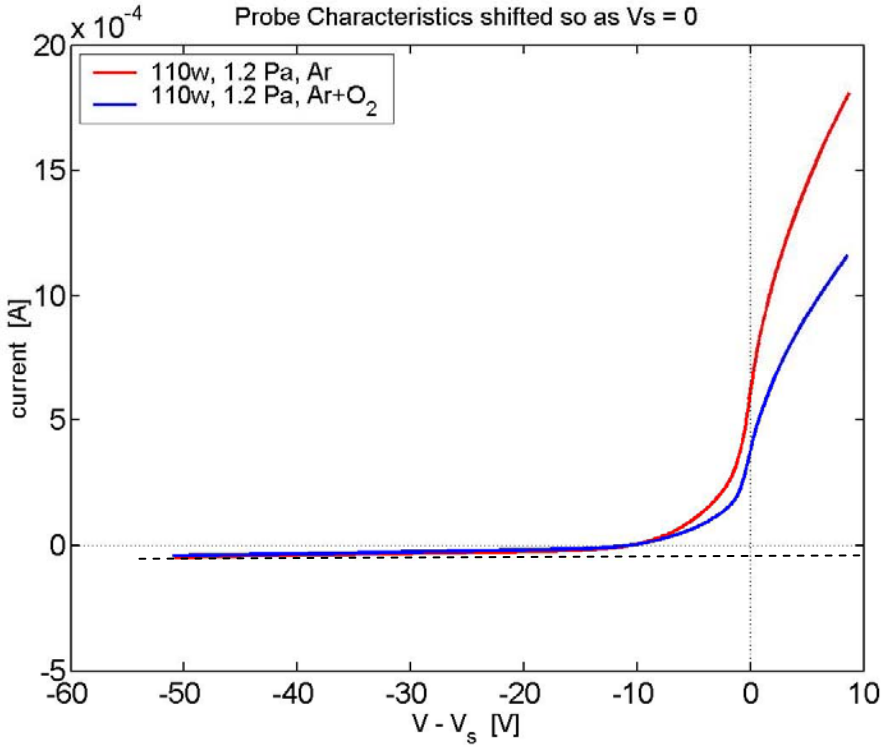

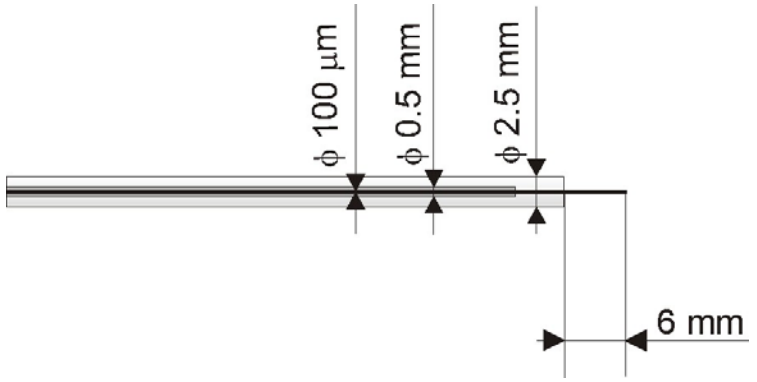

Allows determination of:

- Plasma density
- Floating potential
- Plasma potential
- Electron temperature

Langmuir probe: electron density

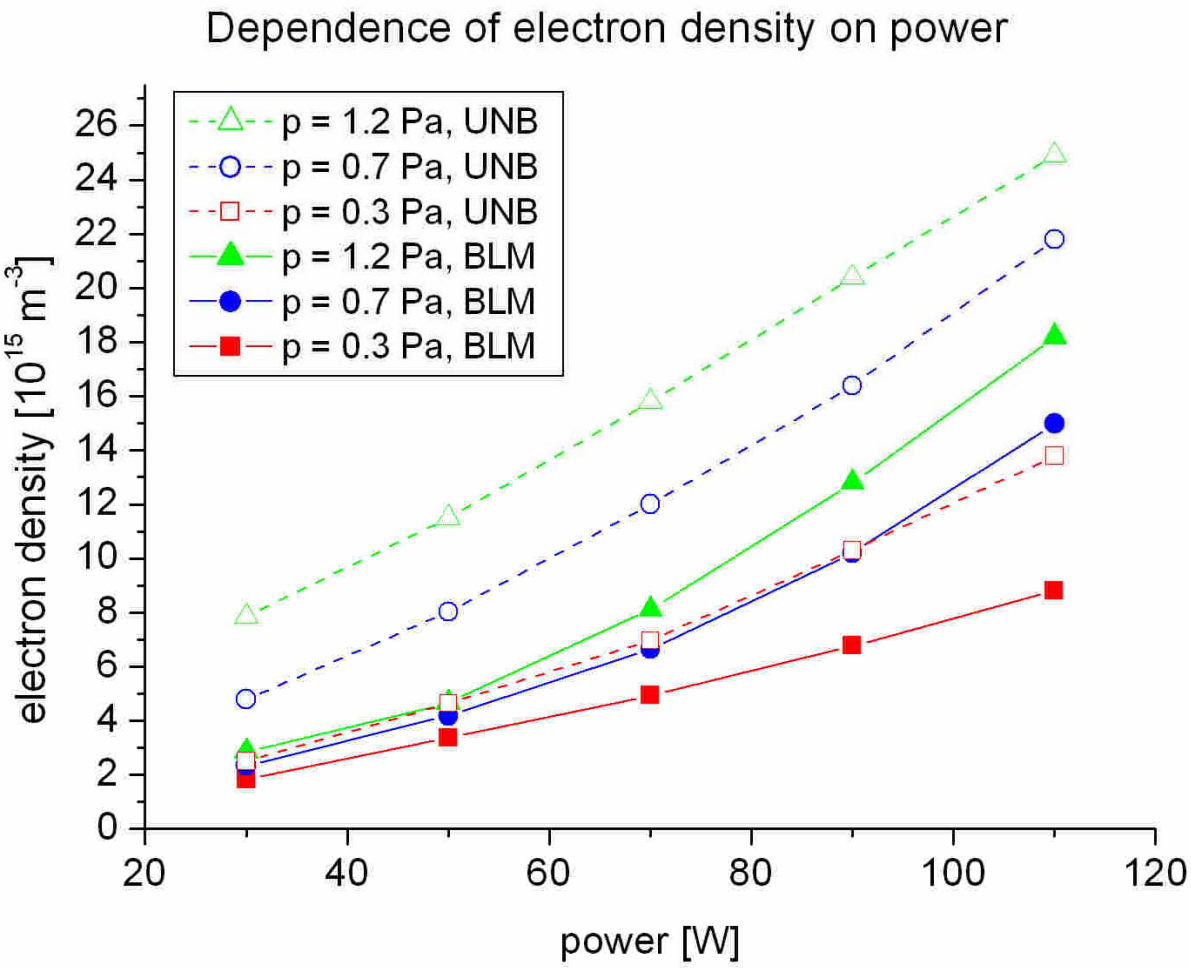

Mean electron energy

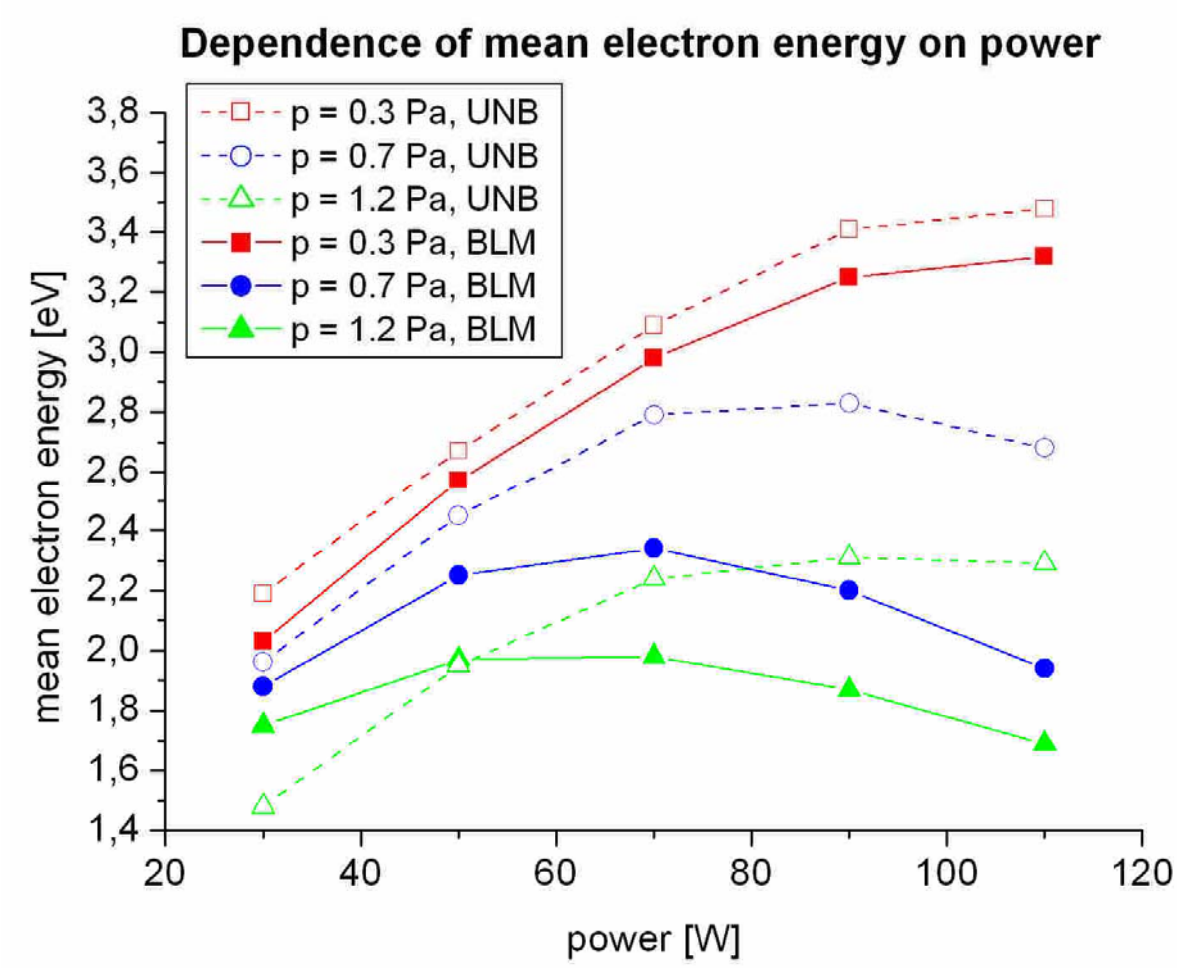

Decrease caused by „cooling“ due to sputtered metal atoms

Plasma diagnostics: Energy-resolved mass spectrometry

Plasma process Monitor

- Mass spectrometer
- Energy filter

Ion energy distributions

Target: In/Sn (9:1)

Ar: 20 sccm; O_2: 2 sccm

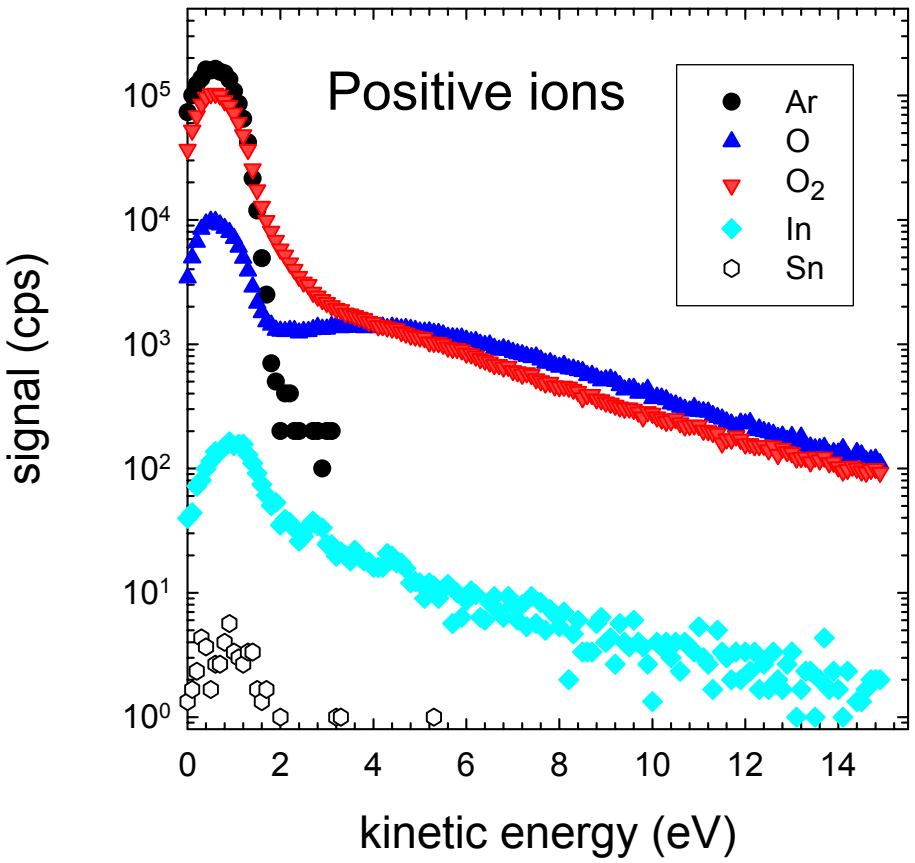

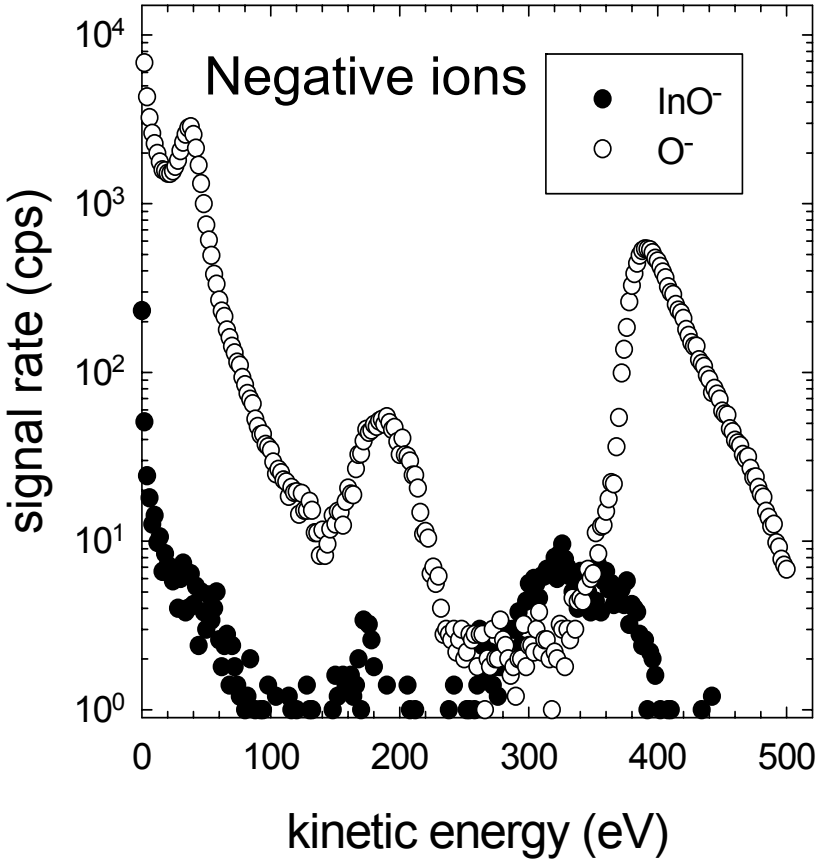

Ion energy distribution of Ti^+ ions vs. pressure

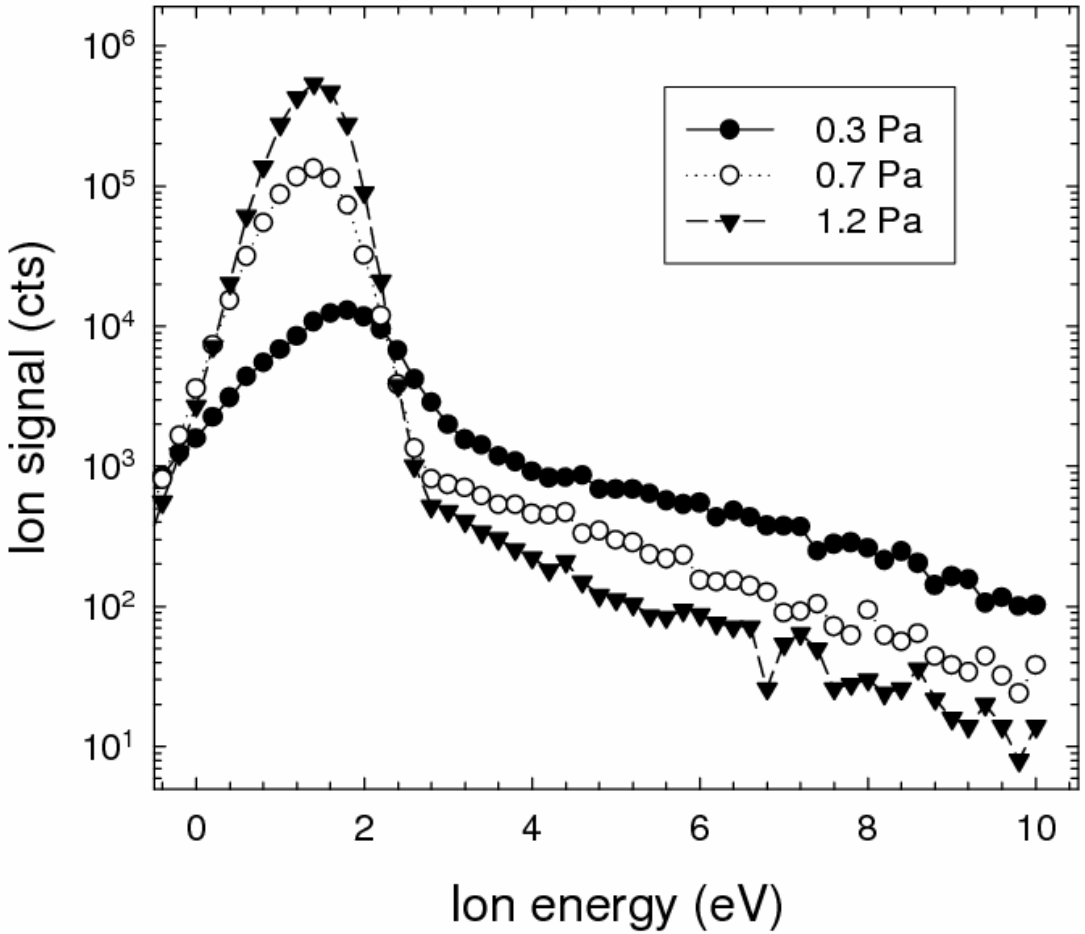

High-energy tail of sputtered metal atoms

Inreased „cooling“ at larger pressures

Thin film deposition
Characterisation of thin films

- Photo electron spectroscopy (XPS)
  - Probe transfer under vacuum
- X-ray diffractometry (GIXD)
- X-ray reflectometry (GIXR)
- Atomic force microscopy (AFM)

X-ray photo electron spectroscopy

X-ray Photoelectron Spectroscopy (XPS) was developed in the mid 1960s by K. Siegbahn and his research group. K. Siegbahn was awarded the Nobel Prize for Physics in 1981 for his work in XPS. The phenomenon is based on the photoelectric effect outlined by Einstein in 1905 where the concept of the photon was used to describe the ejection of electrons from a surface when photons impinge upon it. The energy of the photoelectrons leaving the sample are given by $E_e = E_{Photon} - I$

where *I* is the element-specific electron binding energy.

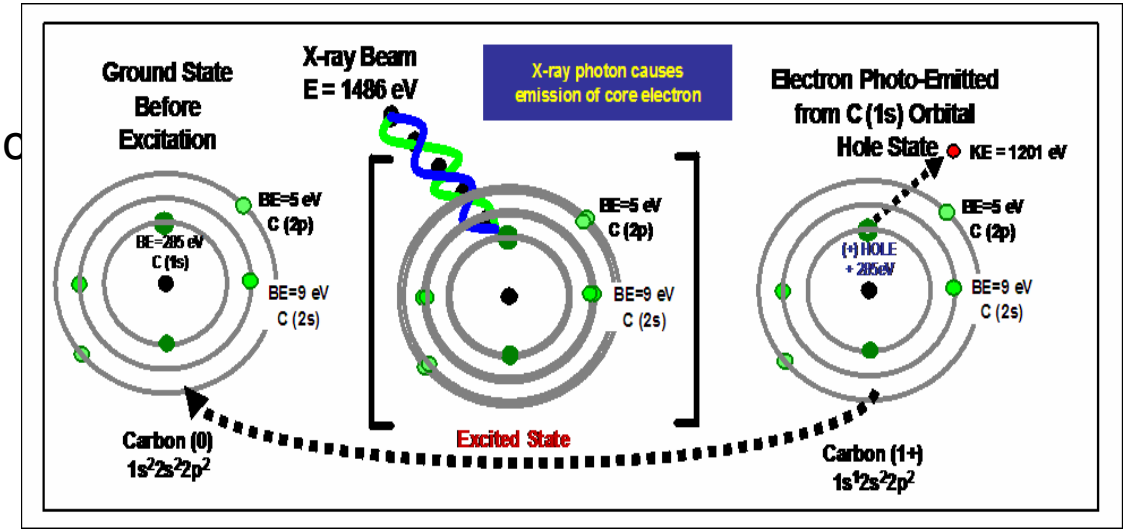

X-ray photo electron spectroscopy

The XPS technique is highly surface specific due to the short range of the photo electrons that are excited from the solid. The binding energy of the peaks are characteristic of each element. The peak areas can be used to determine the composition of the materials surface.

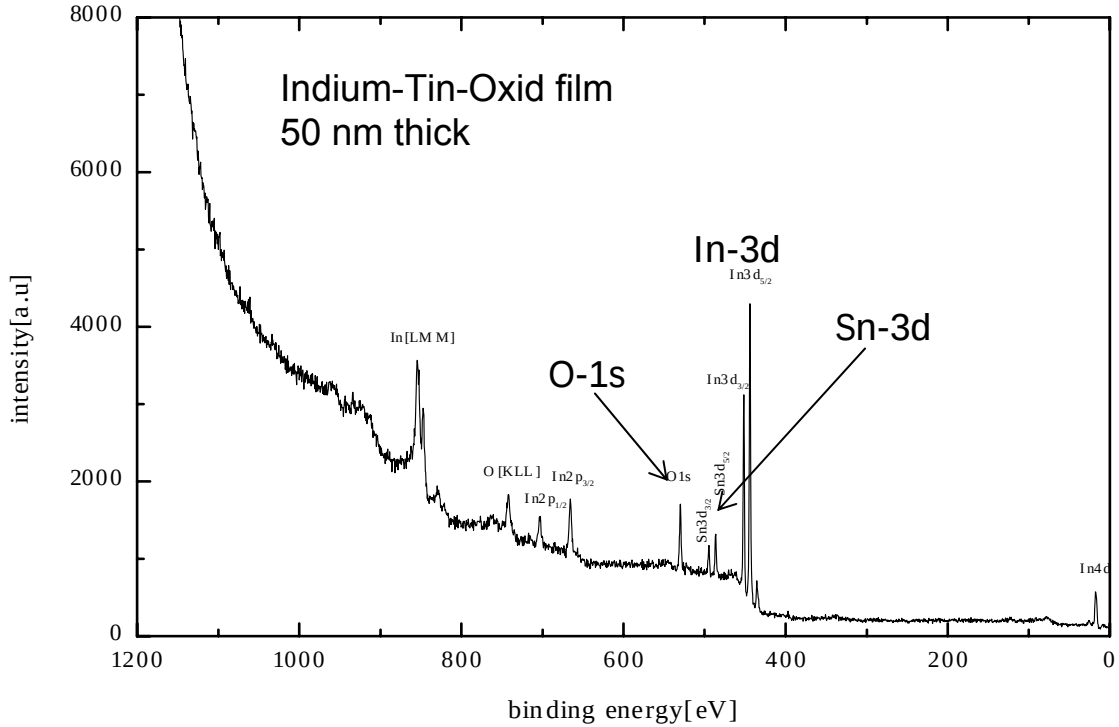

X-ray photo electron spectroscopy

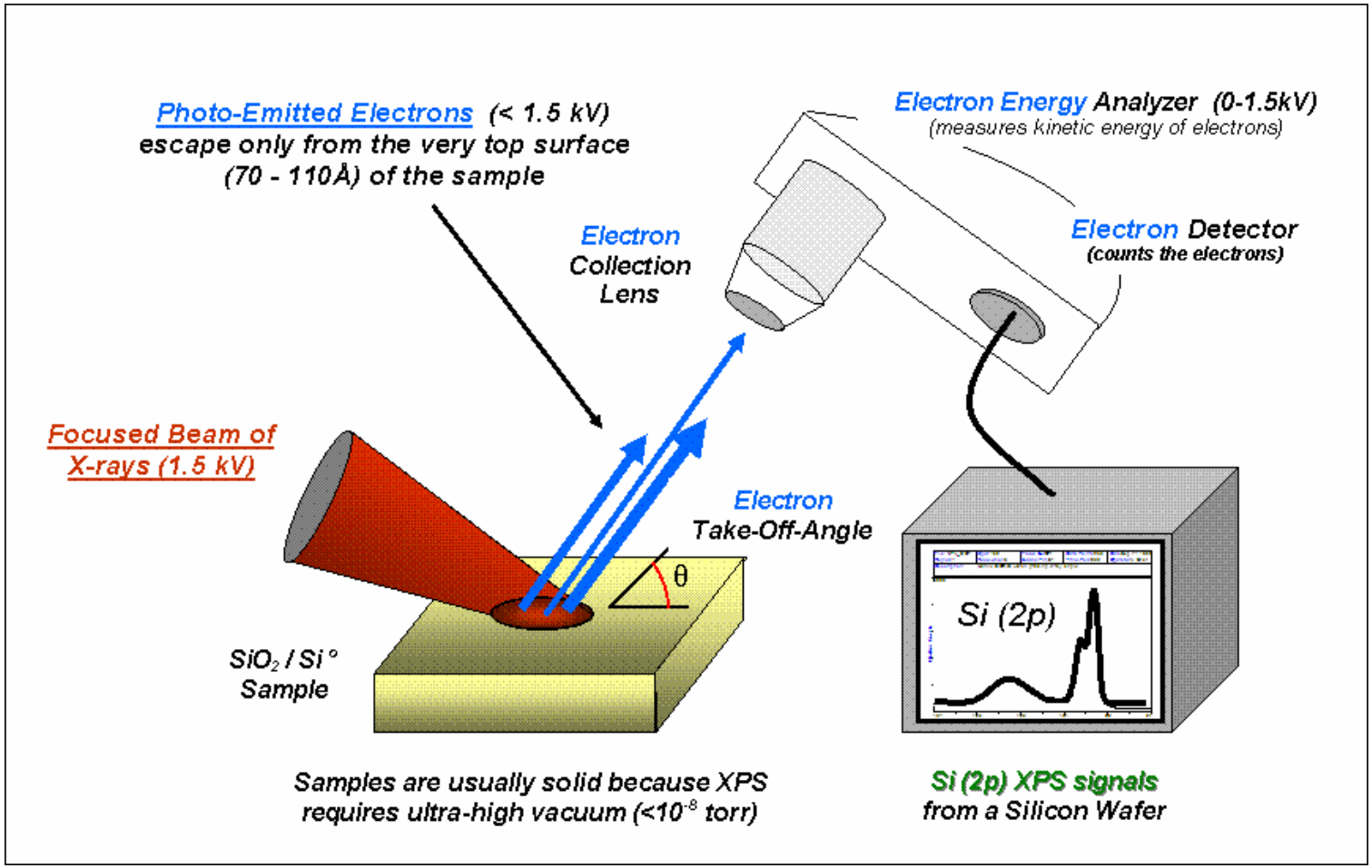

X-ray photo electron spectroscopy

The shape of each peak and the binding energy can be slightly altered by the chemical state of the emitting atom and thus can provide chemical bonding information as well.

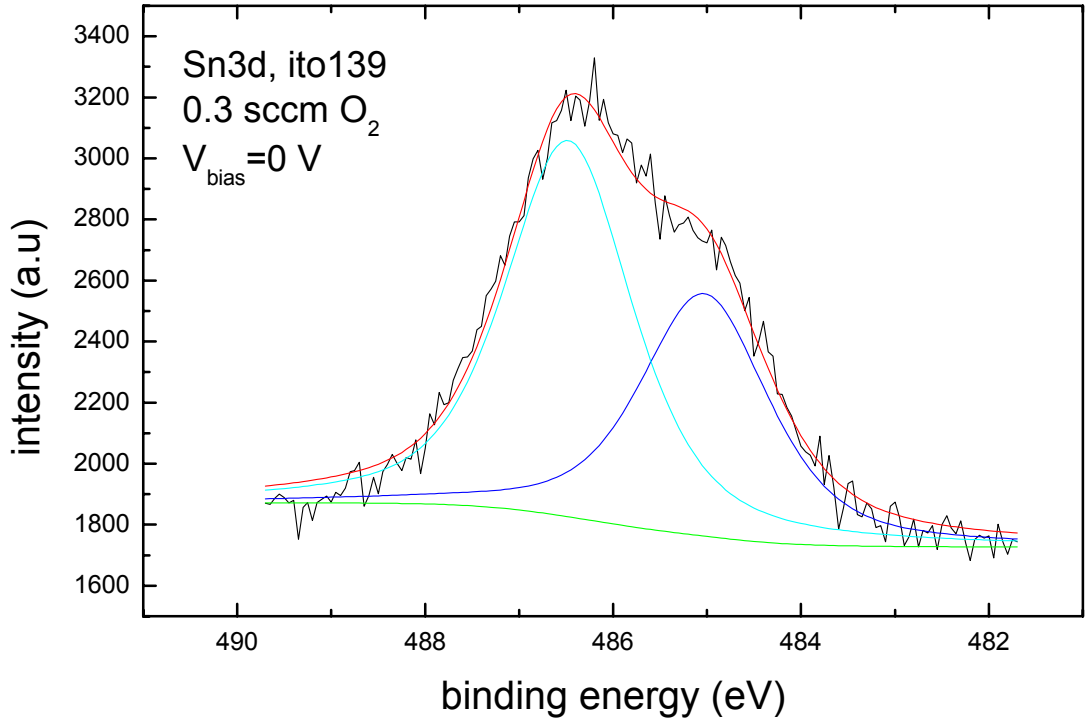

XPS spectrum of Sn-3d peak composed of 2 peaks from metallic Sn and oxidized SnO

Results: XPS: Sn-3d

Variation of O_2 flow

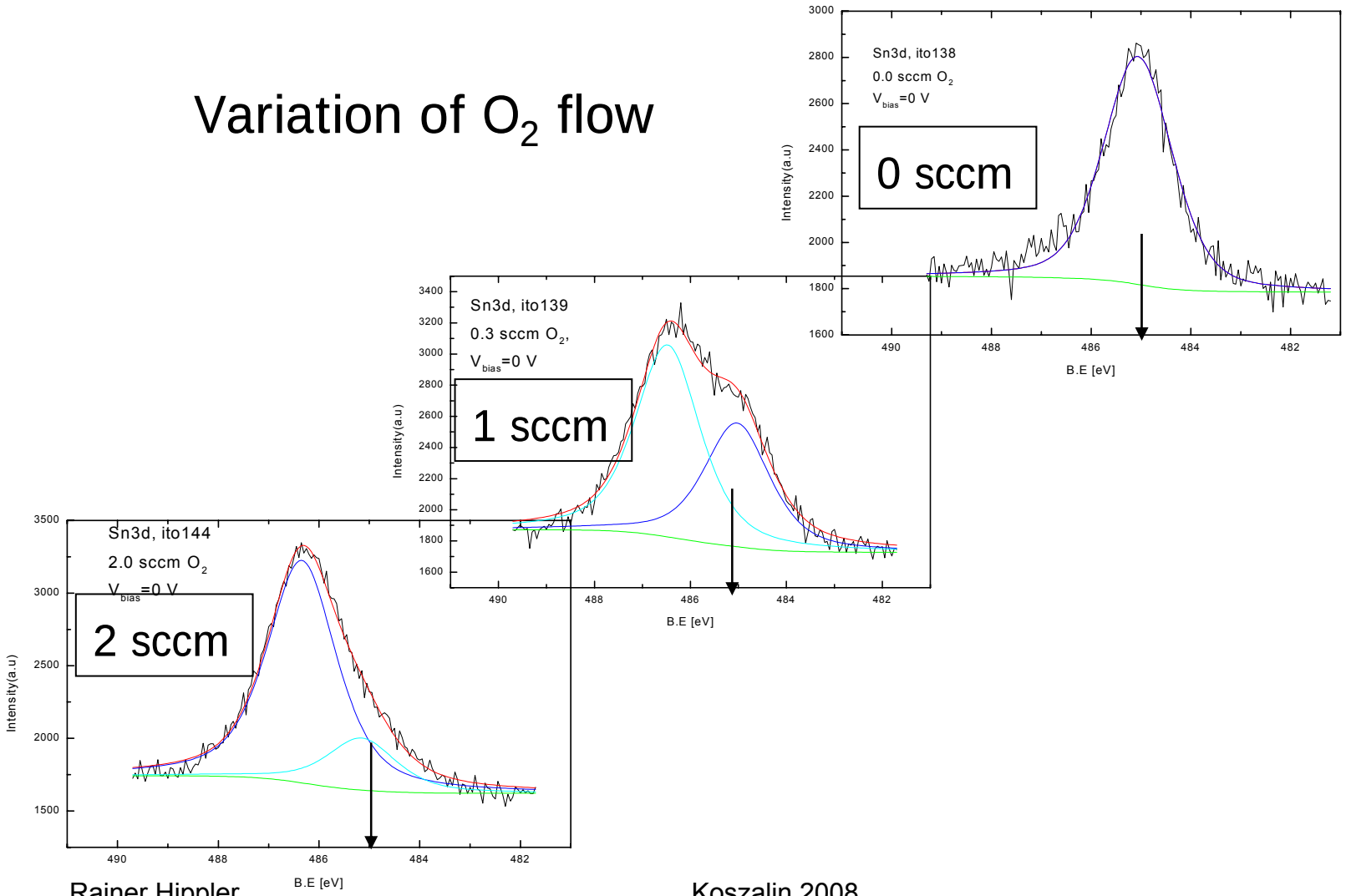

ITO film composition

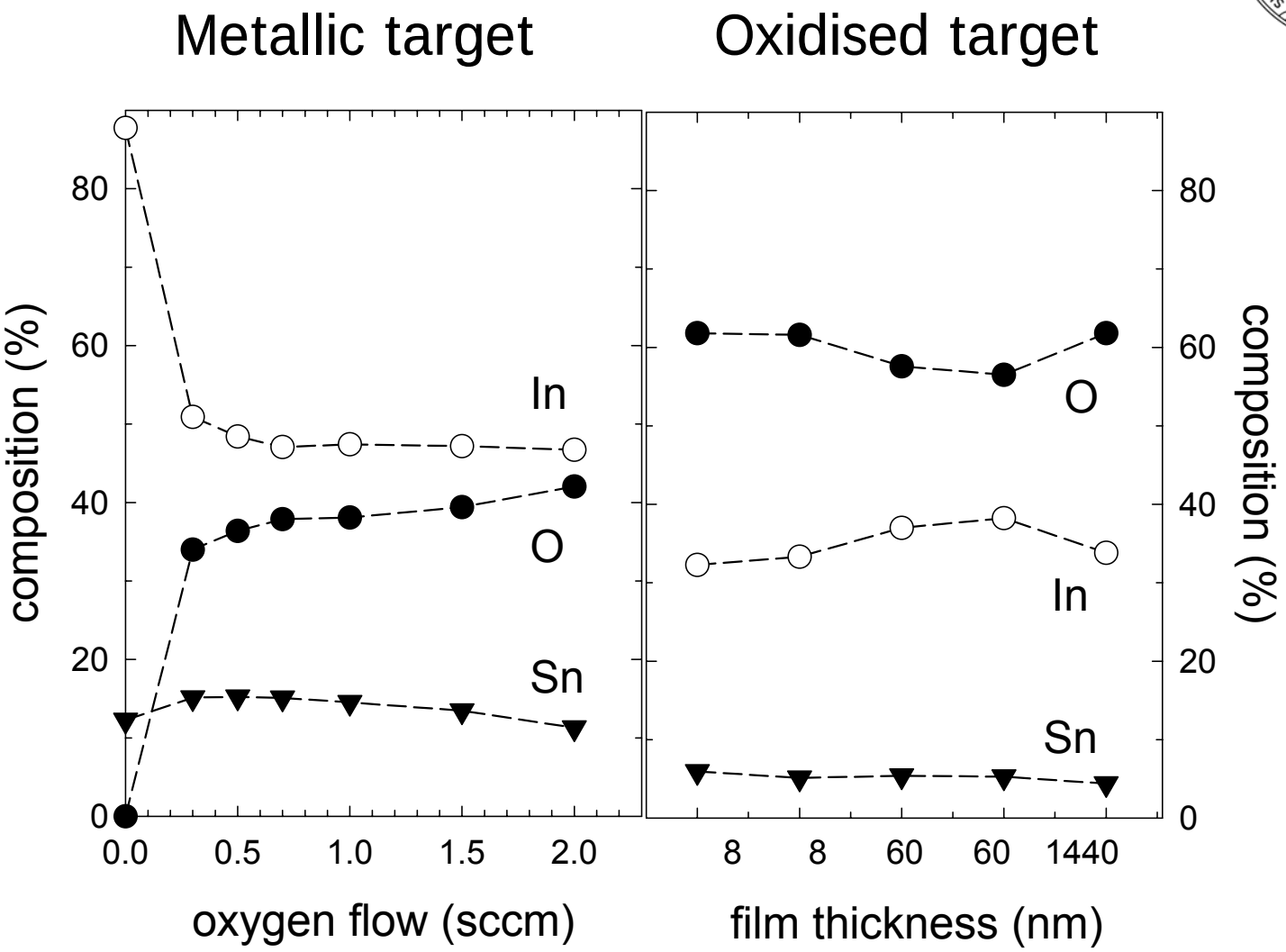

Results: XPS

- Metallic target
  - Oxygen-poor (ca. 40 %)
  - High tin contents (ca. 15 %)
  - Dependence on substrate bias
  - 2 phases: metallic/In_2O_3 and SnO
- Oxidised target
  - Oxygen-rich (60 % or more)
  - Low tin contents (6 %)
  - In_2O_3 und SnO_2

Results II (GIXD, GIXR, AFM)

- Crystallinity in dependence on
  - Oxygen flow
  - Substrate bias
- Deposition rate and density in dependence on
  - Oxygen flow

X-Ray diffractometry (GIXD)

No substrate bias (0 V)

With substrate bias (-50 V)

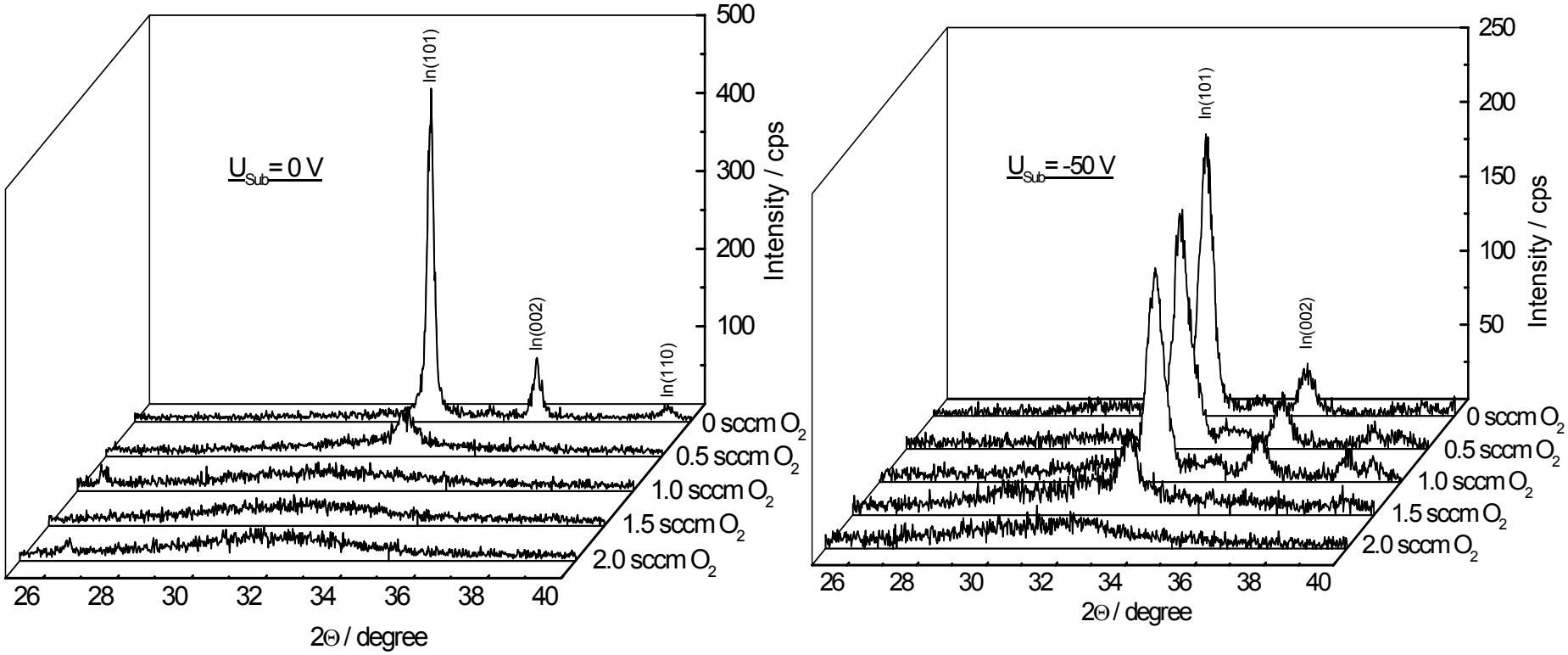

Disappearance of crystalline phase with increasing oxygen flow.
Substrate bias slows down the „disappaearance“.

Atomic Force Microscopy

(a) without O_2

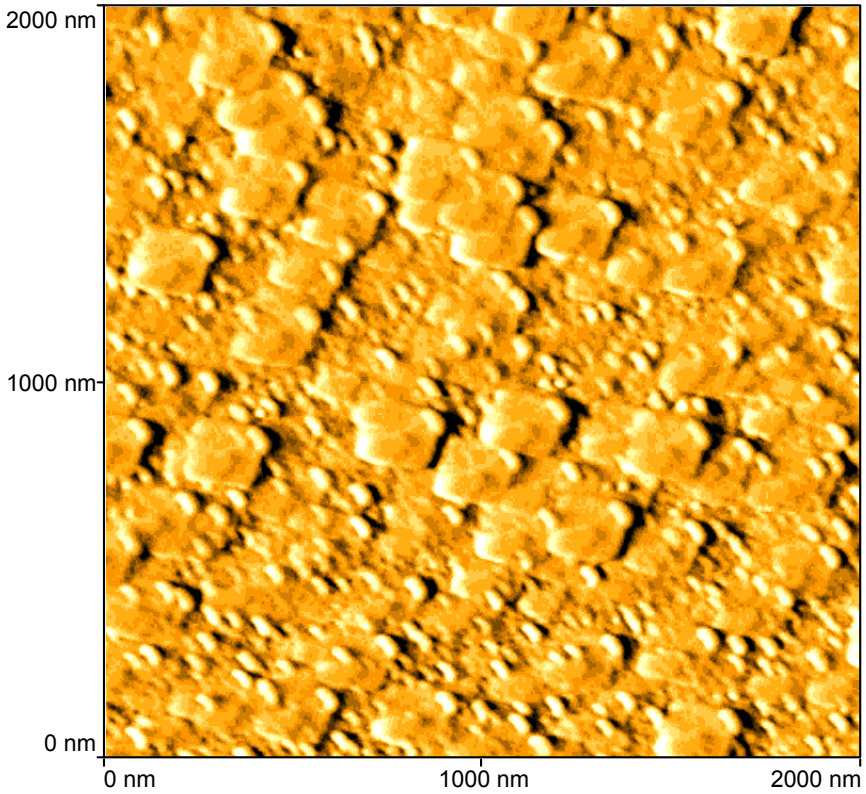

(b) with O_2

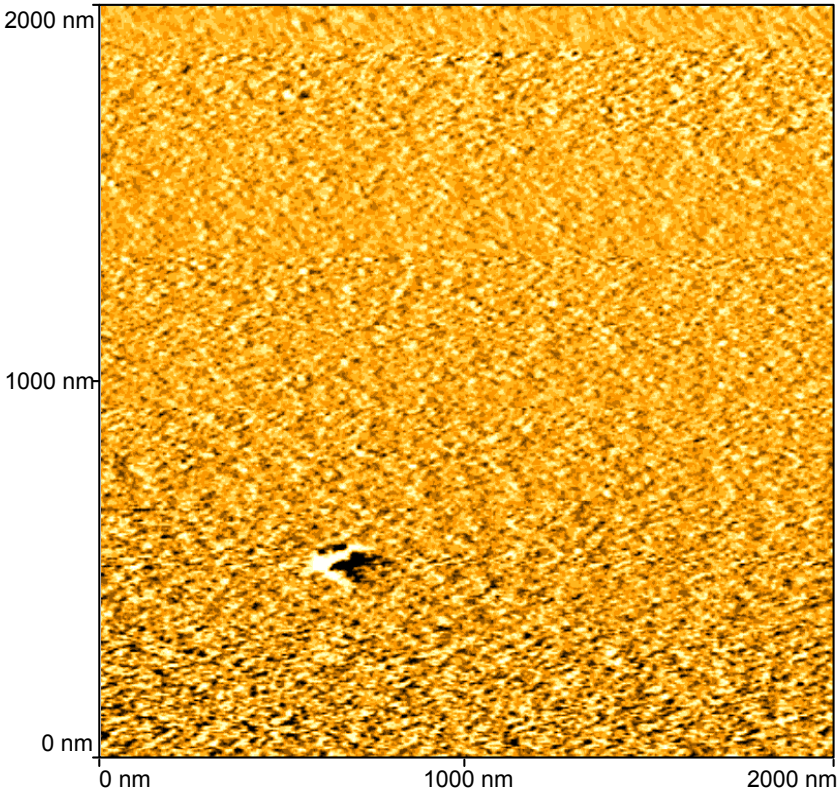

Film composition: XPS and GIXD results

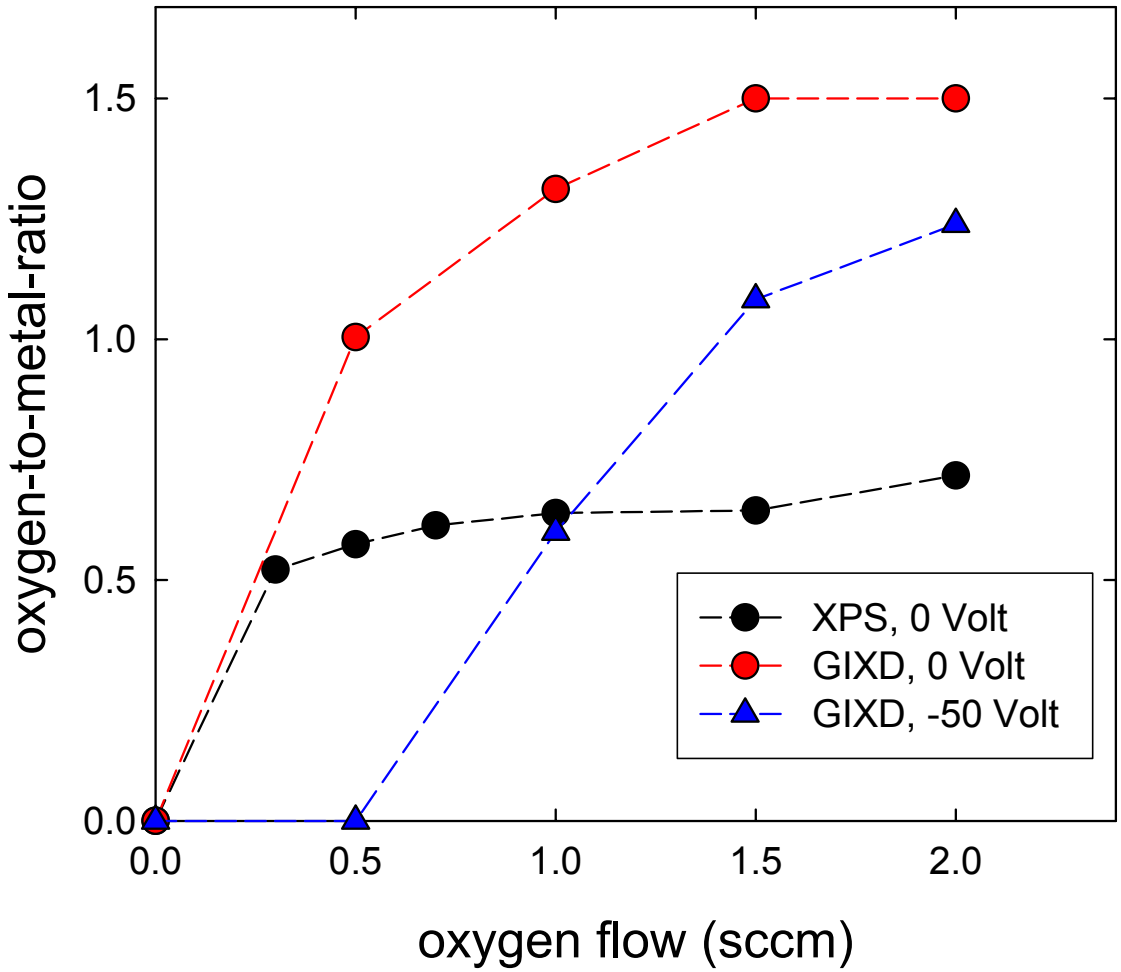

Coexistence of 2 phases:
- ITO (In_2O_3, crystalline)
- Metallic (In, amorpheous)

Indium-tin-oxide target: In/Sn (9:1) with O_2

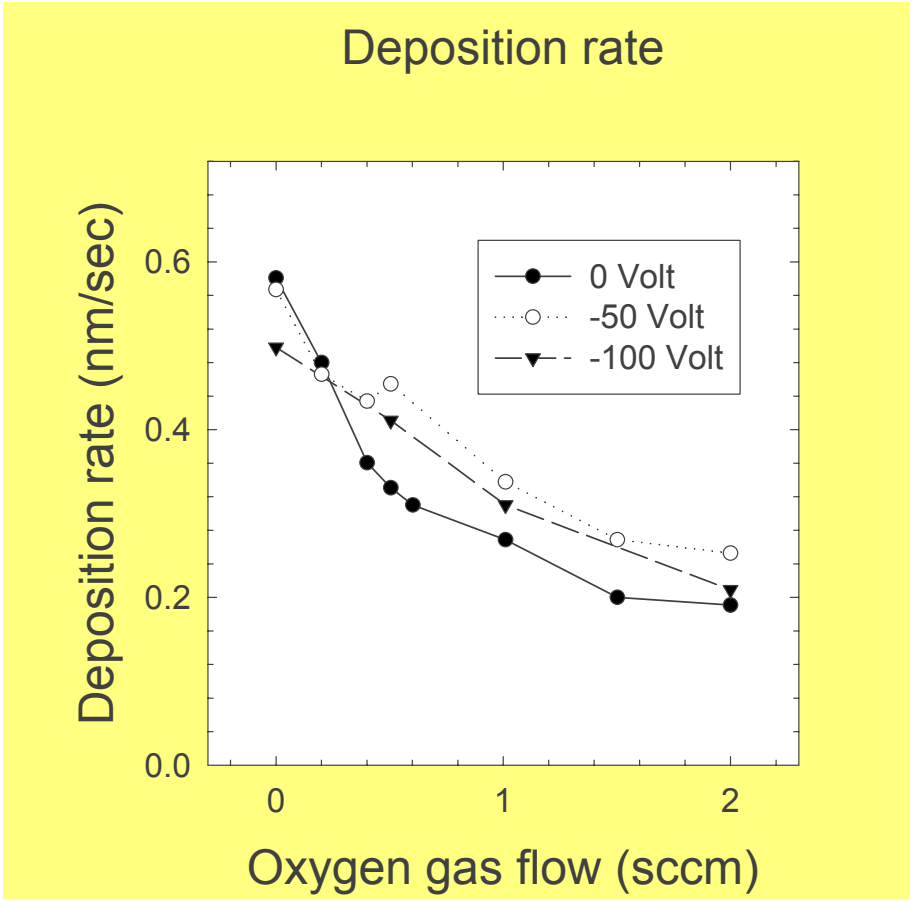

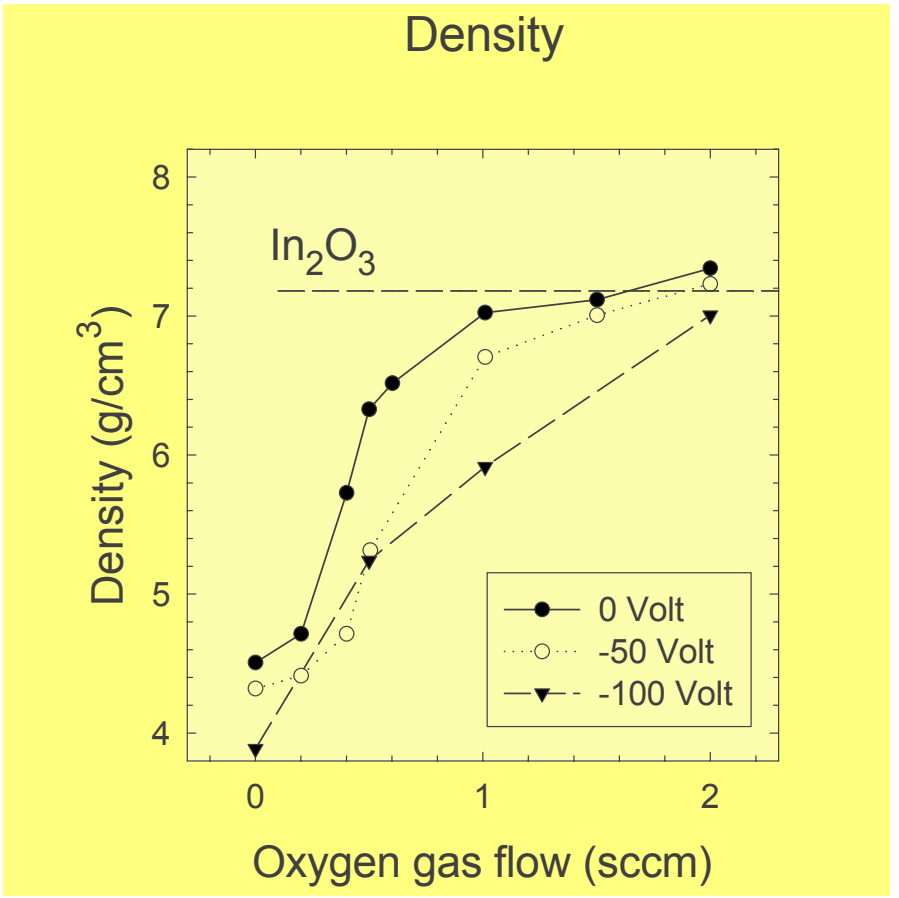

X-ray diffractometry (GIXD)
Post-annealing at 200 °C

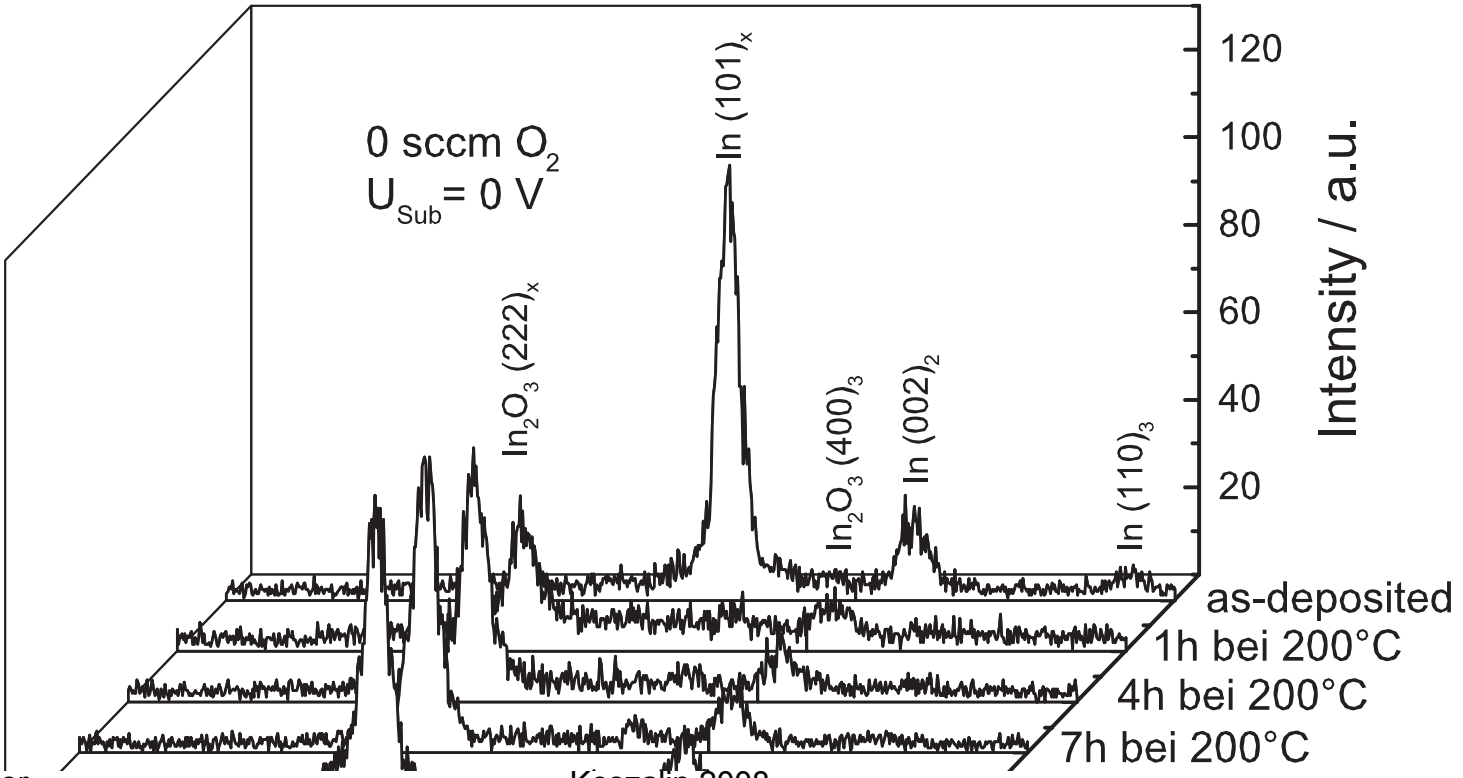

Atomic force microscopy

thickness 50 nm, U_{bias} = 0 Volt

(a) before (b) after annealing (200 ºC)

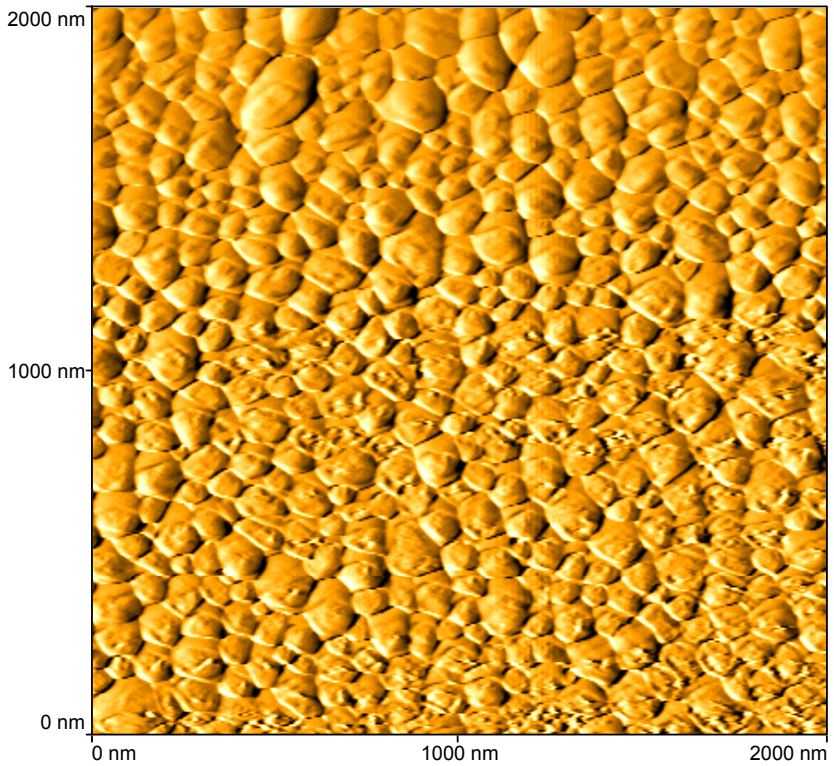

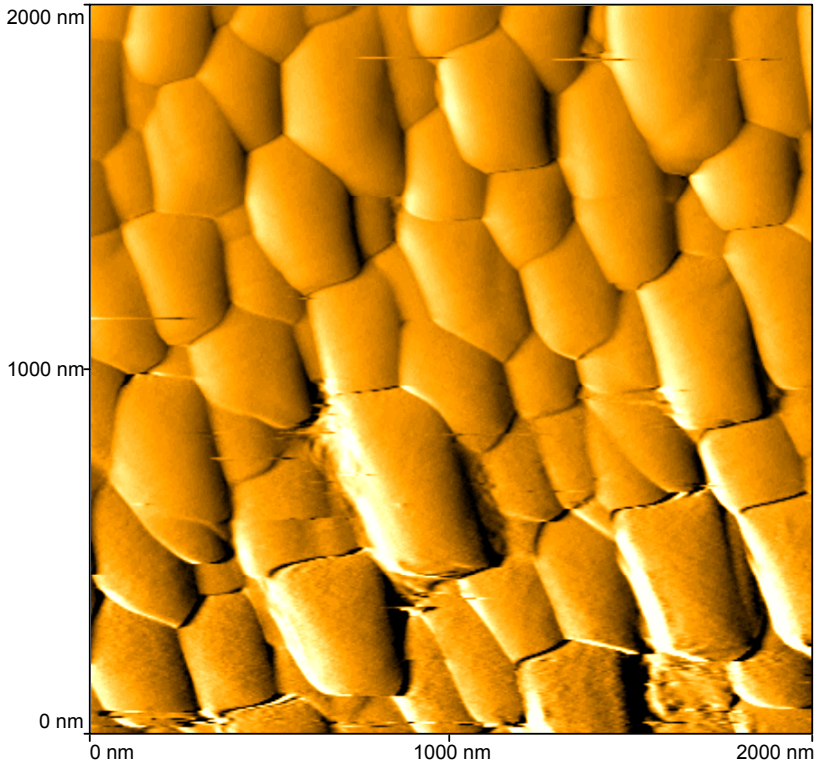

Results

- Disappearance of the crystalline phase (In) with increasing O_2-flow.
- Disappearance depends on substrate bias.
- A complete oxidation is difficult to achieve.
- Deposited films from the metallic target consist of metallic In/Sn or In_2O_3 and SnO.
- Deposition rate, density and morphology of the deposited films show pronounced variations.

Deposition of TiO_x thin films using pulsed dc planar magnetron system

- TiO_2 has good technological properties
- **photocatalytic activity** → „conversion of solar light into useful chemical energy“
- self-cleaning surfaces, purification of air and water, photocatalytic self-sterilisation, … ...

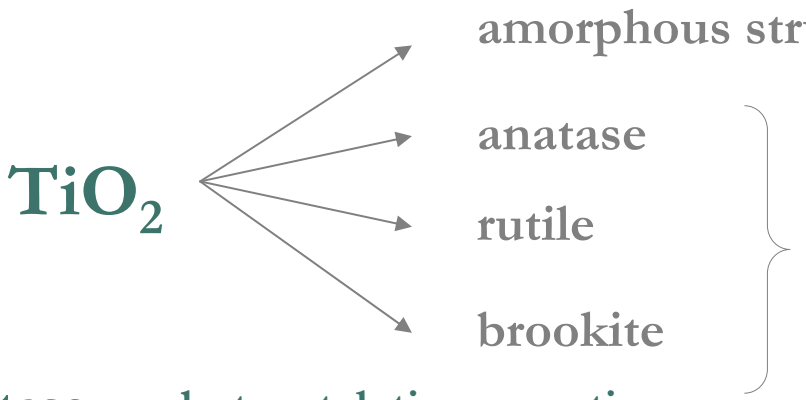

anatase – photocatalytic properties
temperature ~ 300 °C (thermal annealing)

rutile – high refractive index, higher hardness
temperature ~ 900 °C (conversion of anatase)

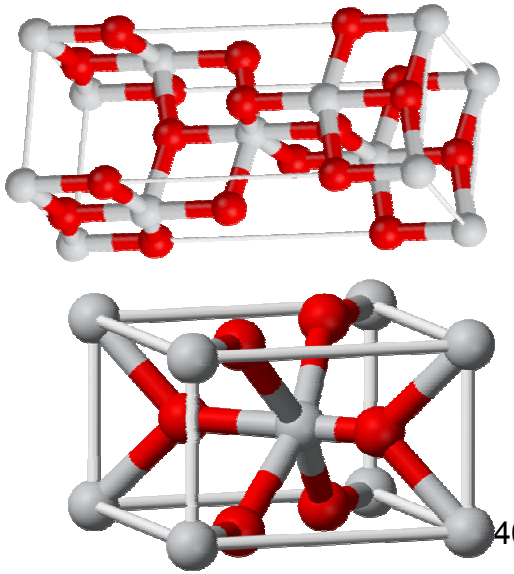

Structure of deposited TiO_2 thin films

- Grazing incidence XRD (Seiffert FPM HZG 4)
- dependence of structure on ratio Ar/O_2 gases and pressure of **„unheated samples“**
- TiO_2 was found in rutile, anatase, and amorphous structure, (α-Titanium)

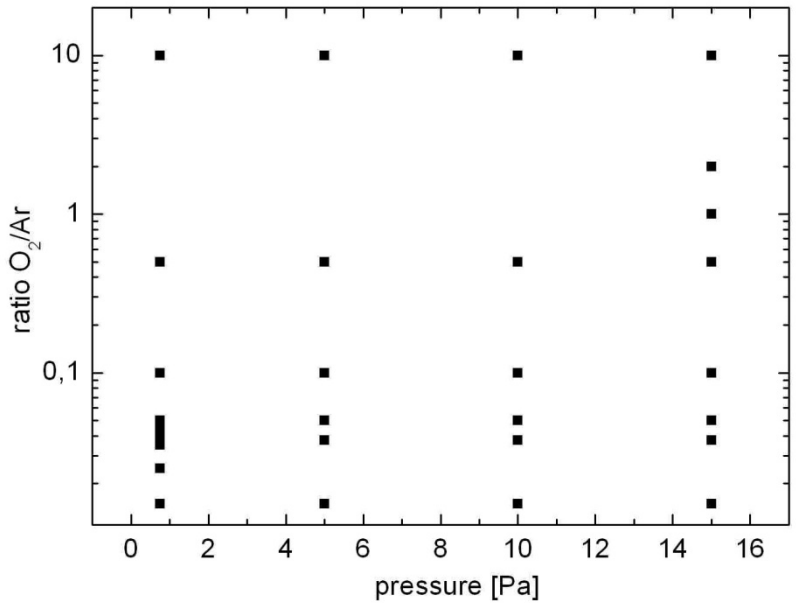

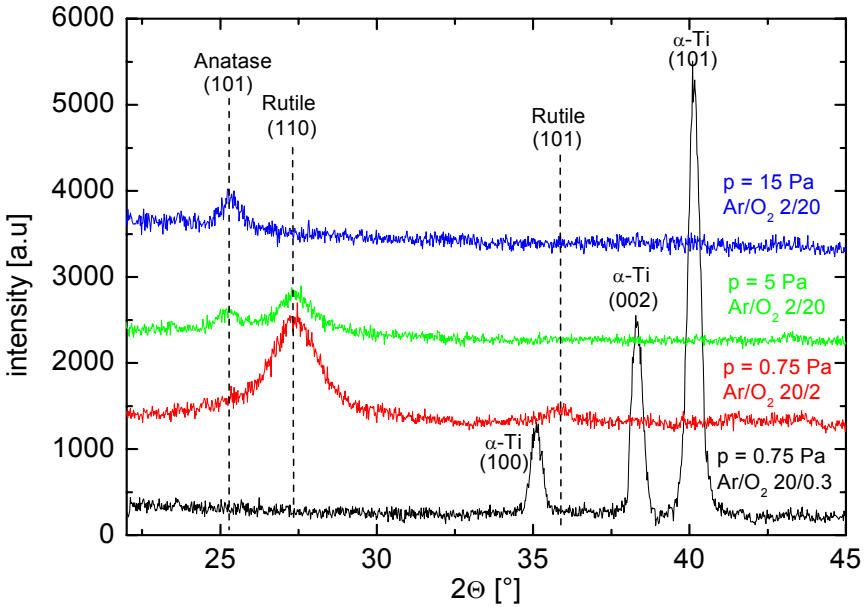

Structures dependencies

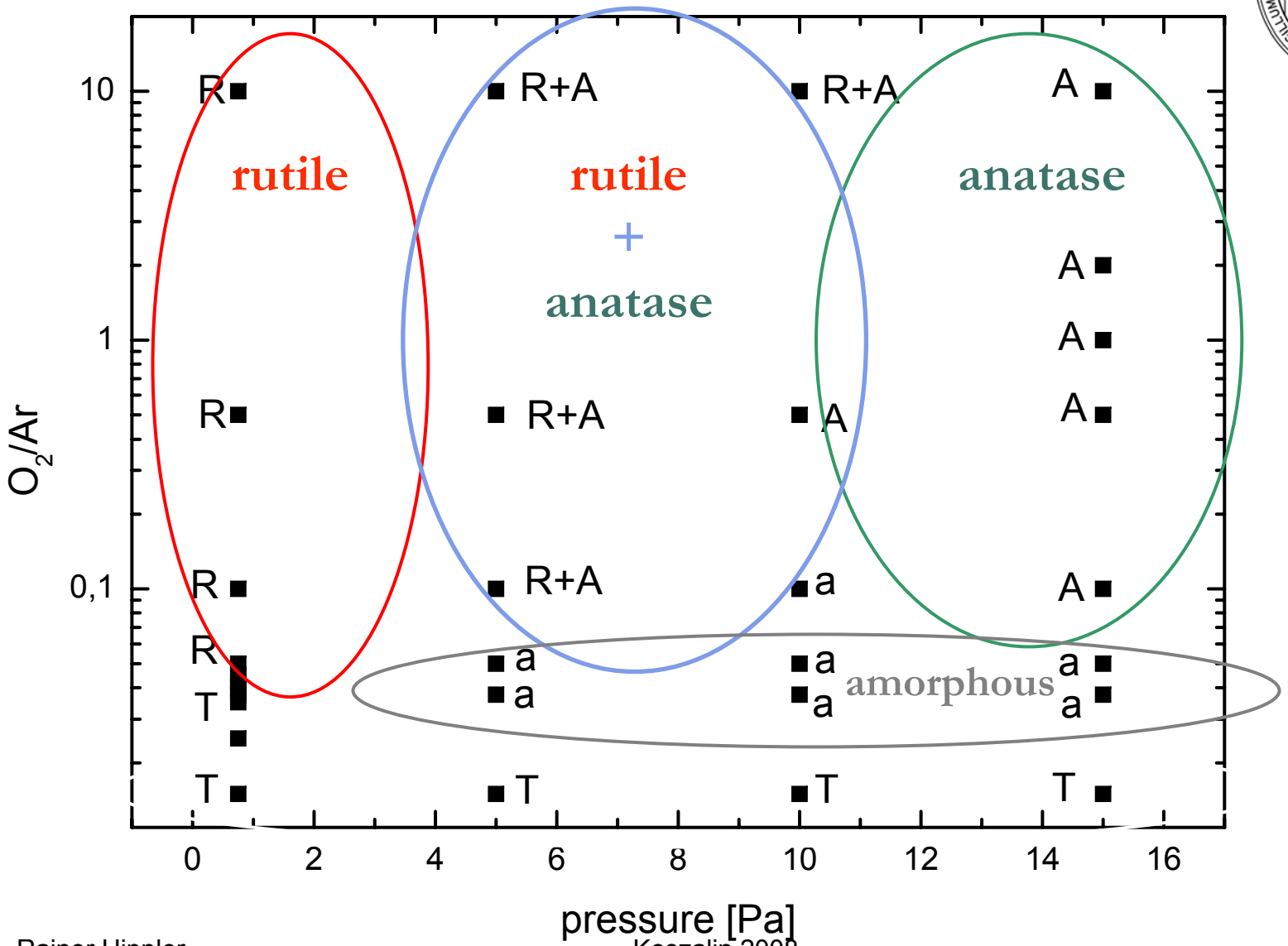

Surface morphology (AFM): Nano-size particles (clusters)

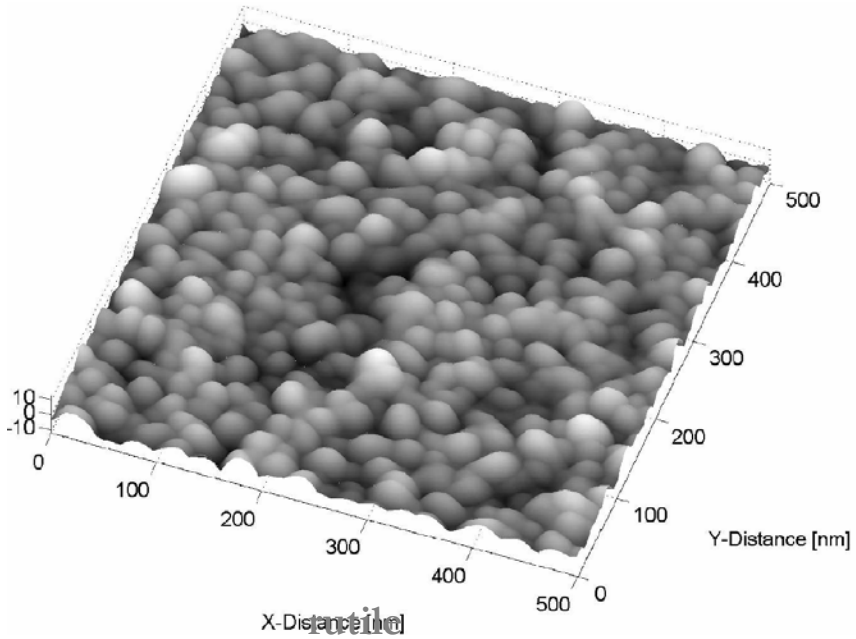

rutile

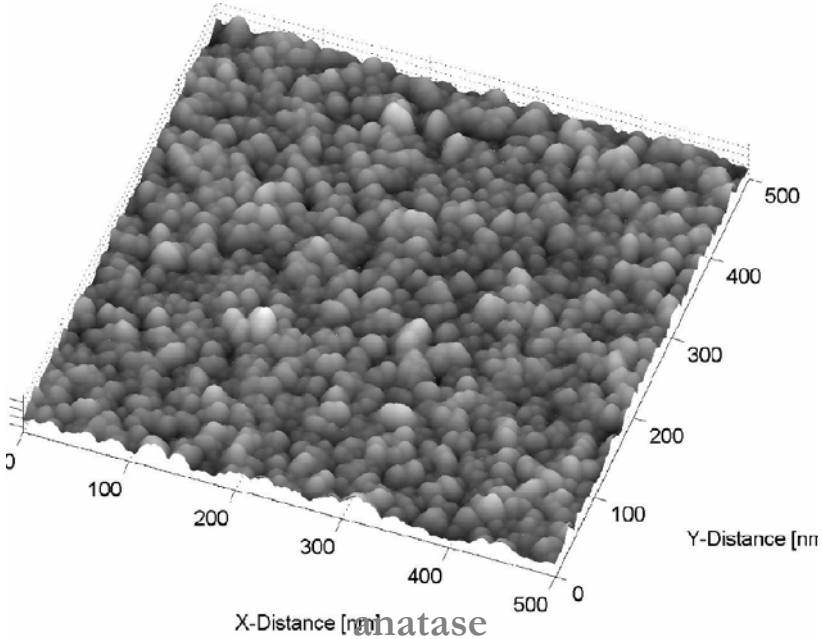

anatase

Dependence of surface structure on pressure and/or crystalline phase

measured cluster radius – rutile 15.40 nm, anatase 10.25 nm

measured cluster surface – rutile 783.1 nm^2, anatase 330.8 nm^2

How to produce nano-size particles?

Particle formation in plasmas.
Mass spectra of positive ions: Ar/CH_4 vs. Ar/C_2H_2)

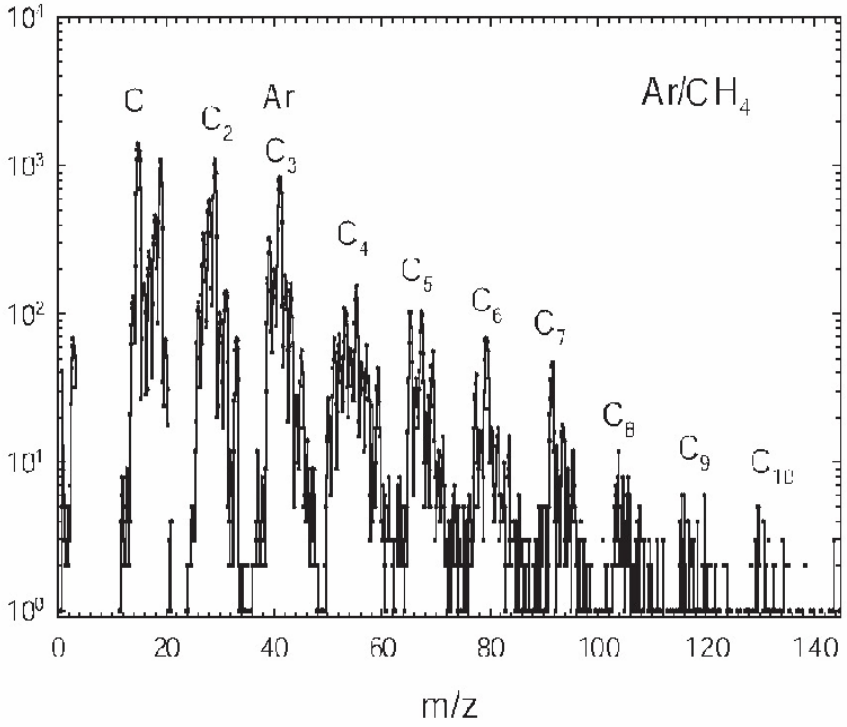

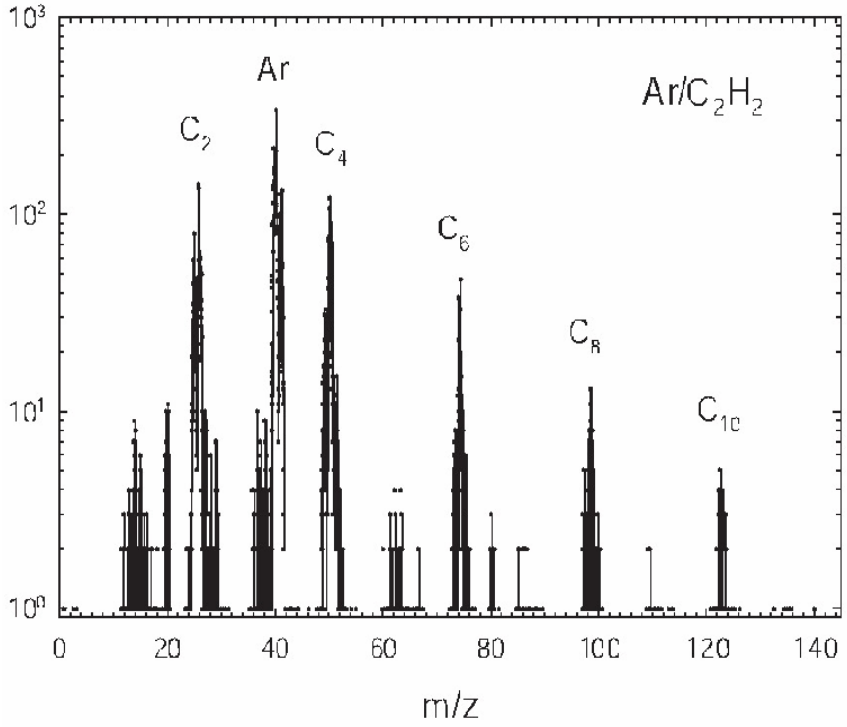

H.T. Do, G. Thieme, M. Fröhlich, H. Kersten, R. Hippler,
Contrib. Plasma Phys. 45, 378 – 384 (2005)

Particle nucleation and growth

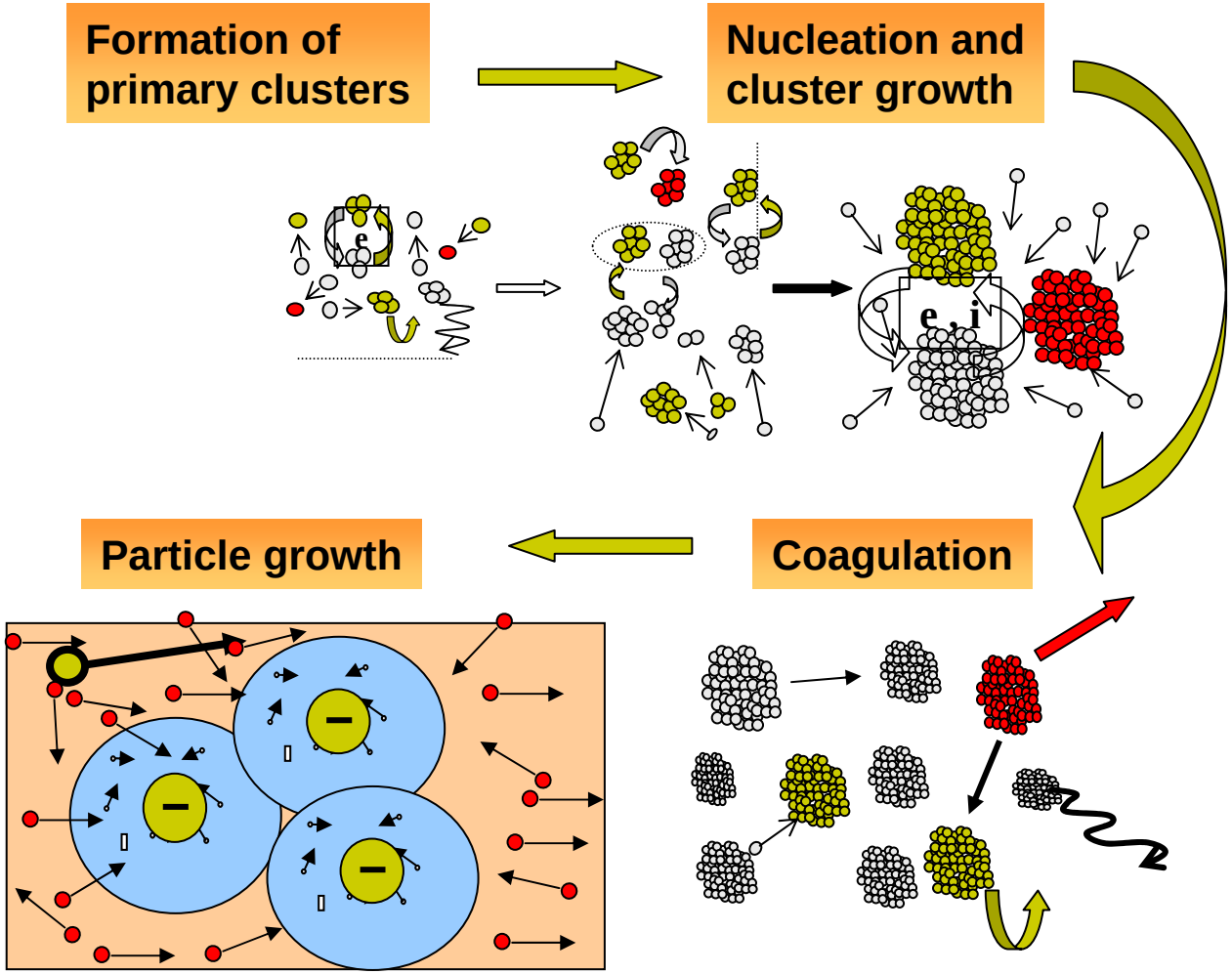

Typical evolution

Nucleation (3-body reaction):

$A + A + X \rightarrow A_2 + X$

Cluster growth (atom adsorption):

$A_n + A \rightarrow A_{n+1}$

Coagulation:

$A_n + A_m \rightarrow A_{n+m}$

C. Hollenstein (Ecole Polytechnique Lausanne, Switzerland)

Nano-size particle formation

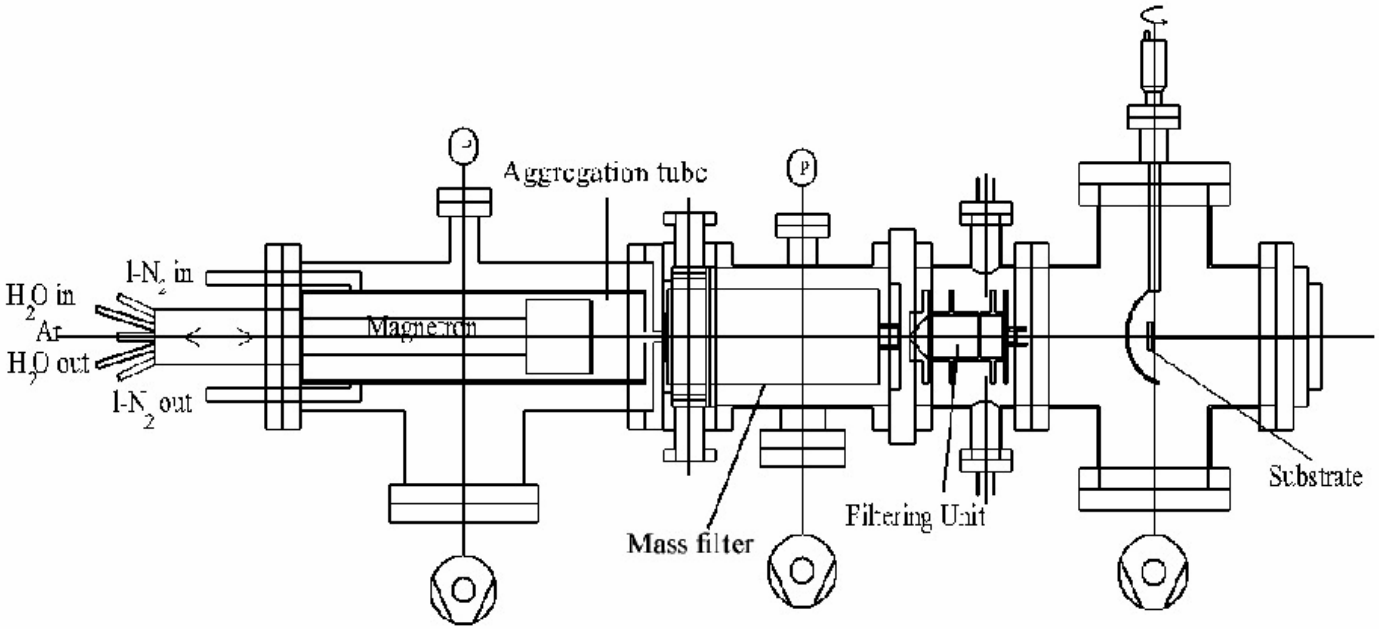

Nano-size particle growth from sputtered atoms in a magnetron discharge

Depostion of nano-size particles on surfaces

Ion energy distribution of Ti^+ ions vs. pressure

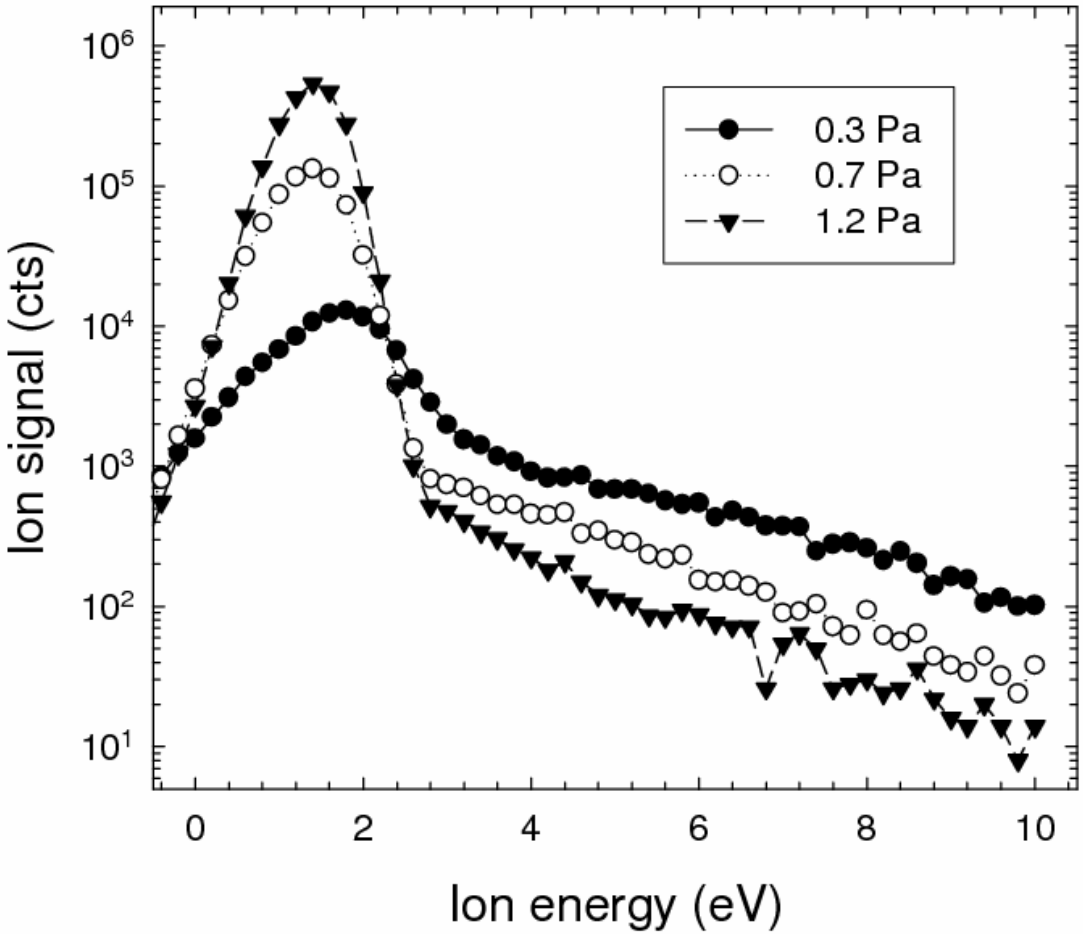

High-energy tail of sputtered metal atoms

Inreased „cooling“ at larger pressures.

Cooling leads to an increase of cluster formation.

Nano-size Ag particles on Si(100)

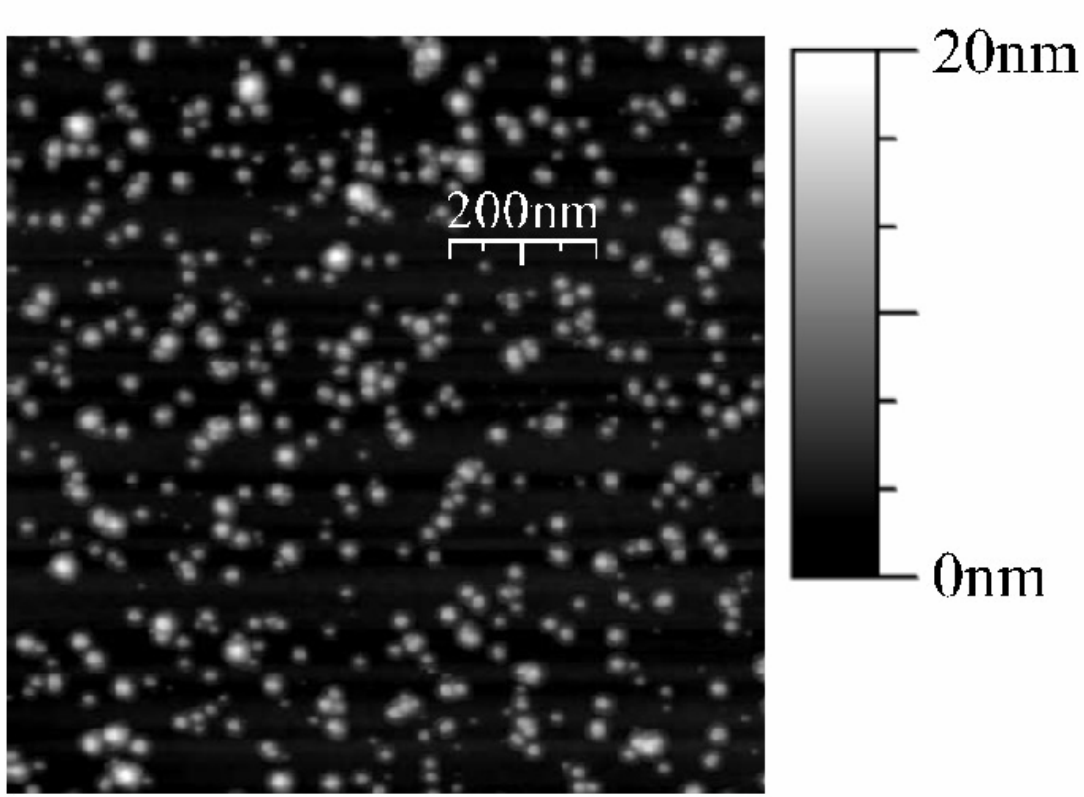

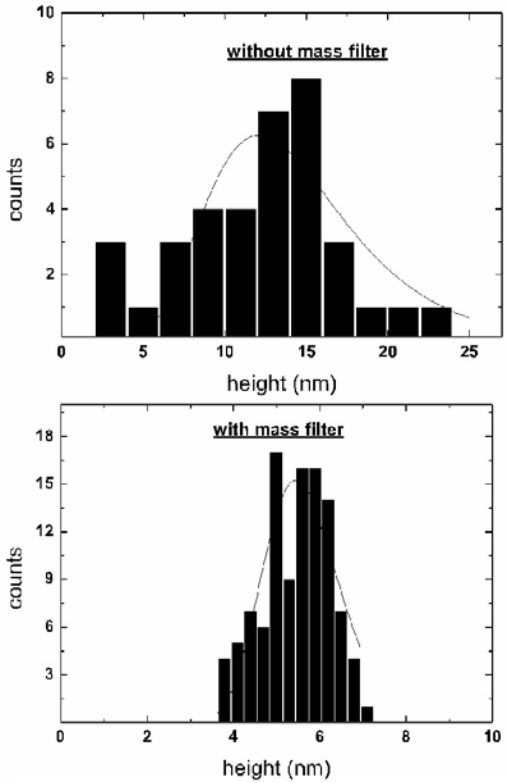

Size distribution of deposited Ag clusters with and without mass filter.

I. Shyjumon, M. Gopinadhan, O. Ivanova, M. Quaas, H. Wulff, C.A. Helm, R. Hippler, EJP D (2006)

Melting of deposited nano-size Ag clusters

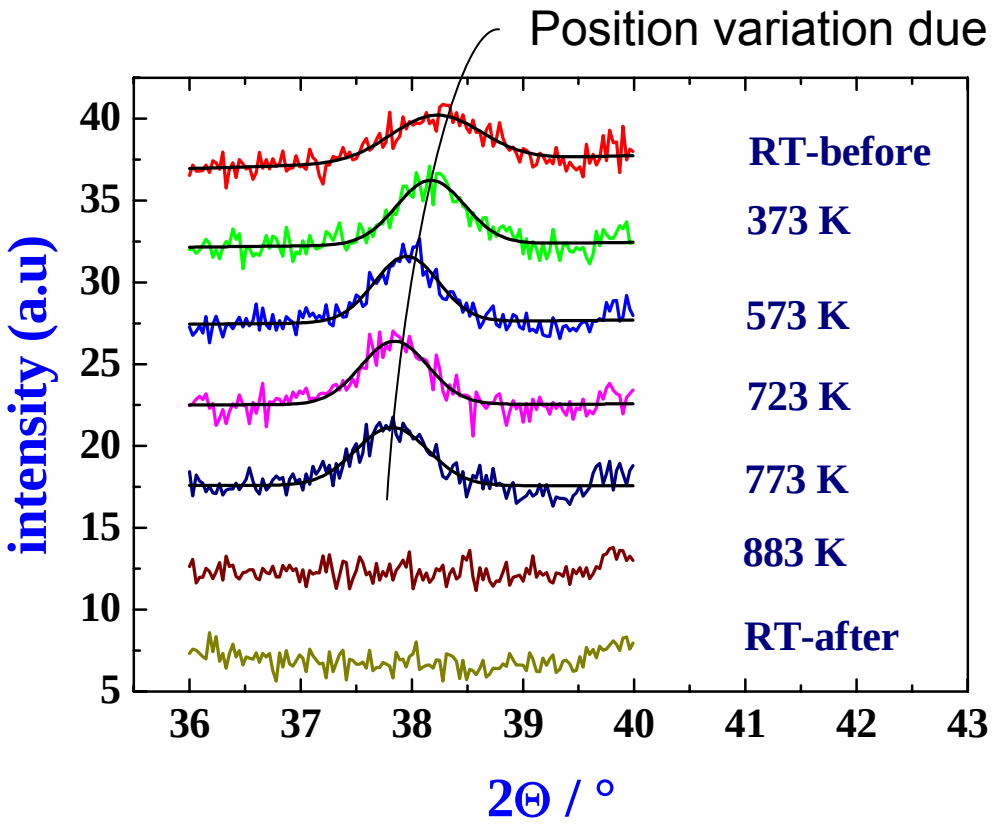

$$\Delta T = \frac{4\sigma M T_{bulk}}{\Delta H_m r \rho}$$

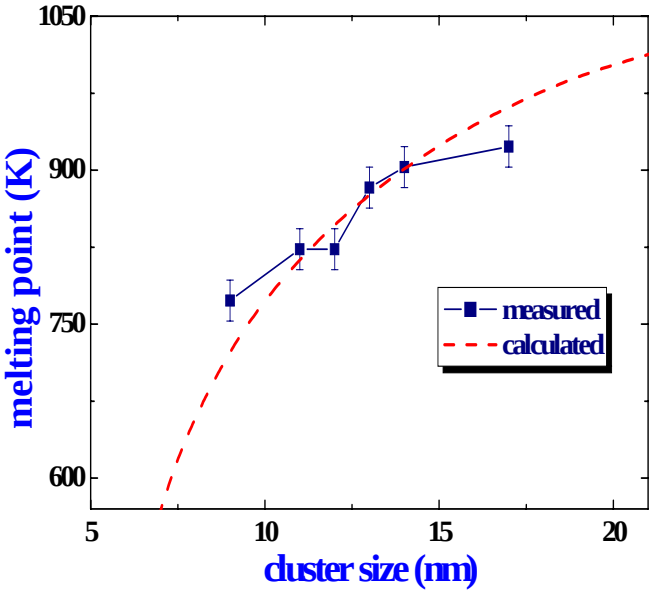

Cluster size dependence on time

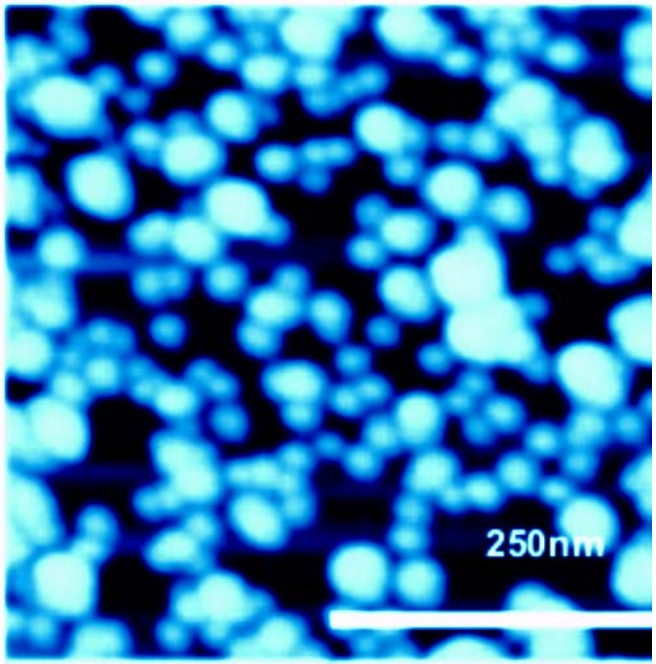

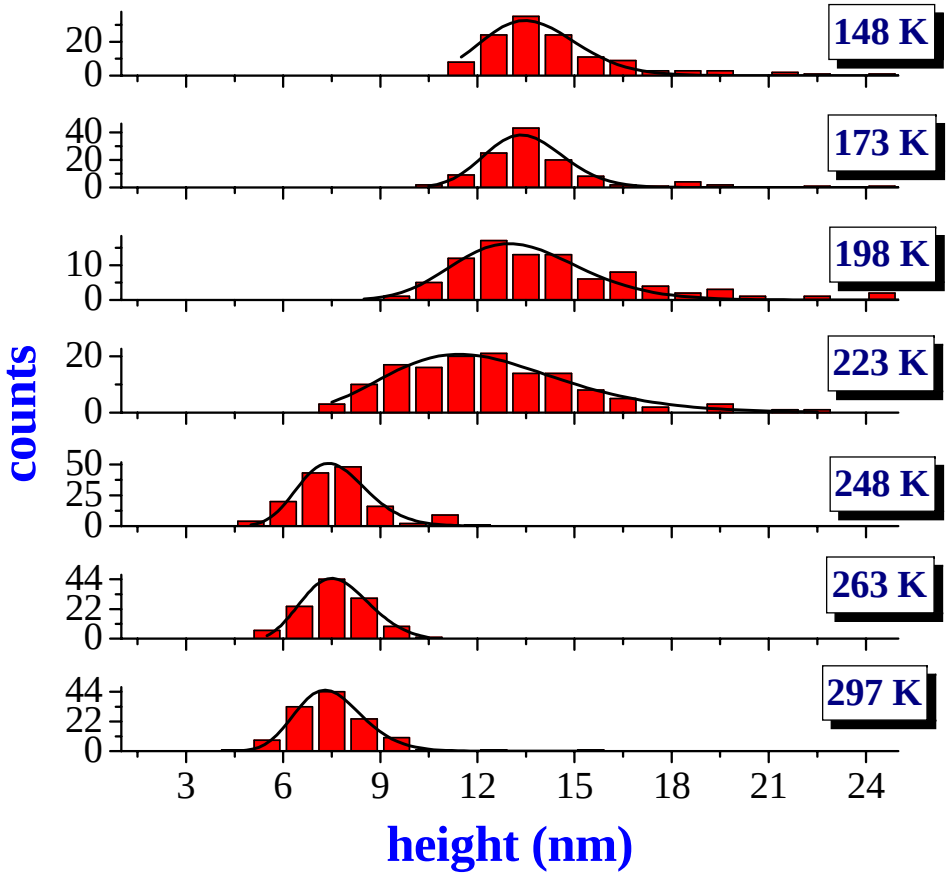

N/µm^2 - 280 to 390

14 to 24 nm

Cluster size dependence on time

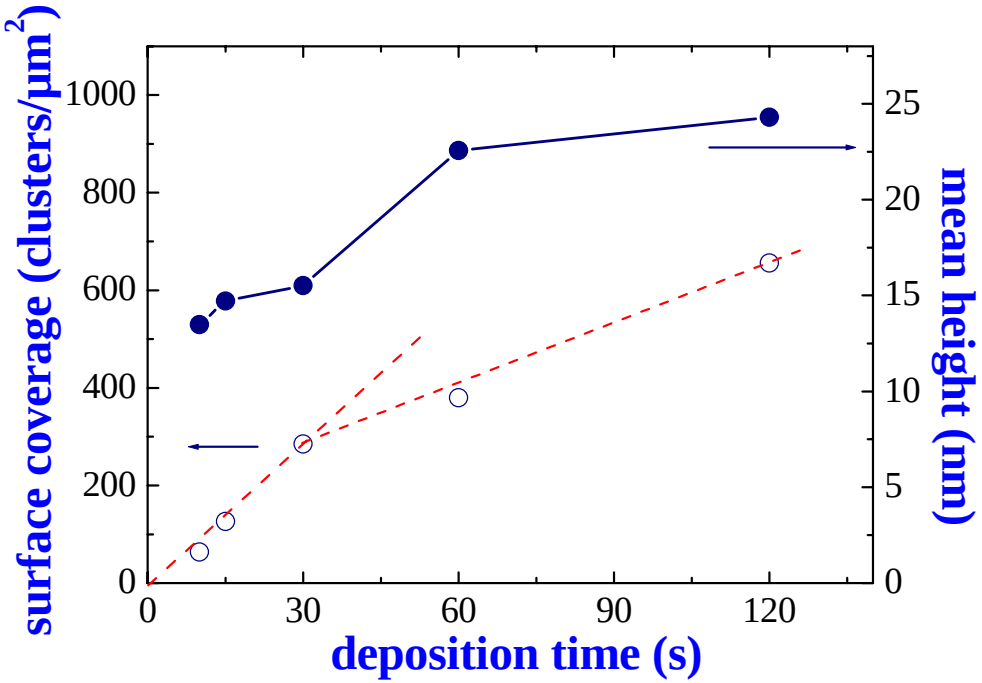

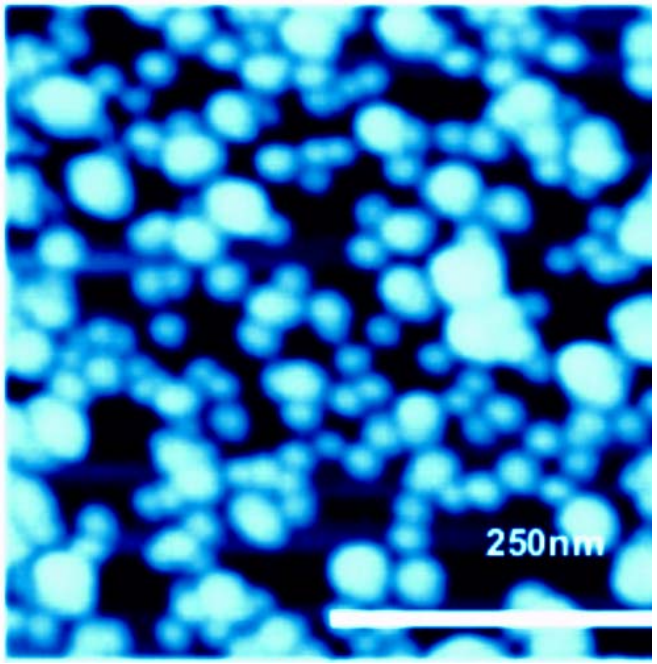

Around 30 s, the second layer growth - starts before the first layer is completed

N/μm² - 280 to 390
14 to 24 nm

Chemical composition

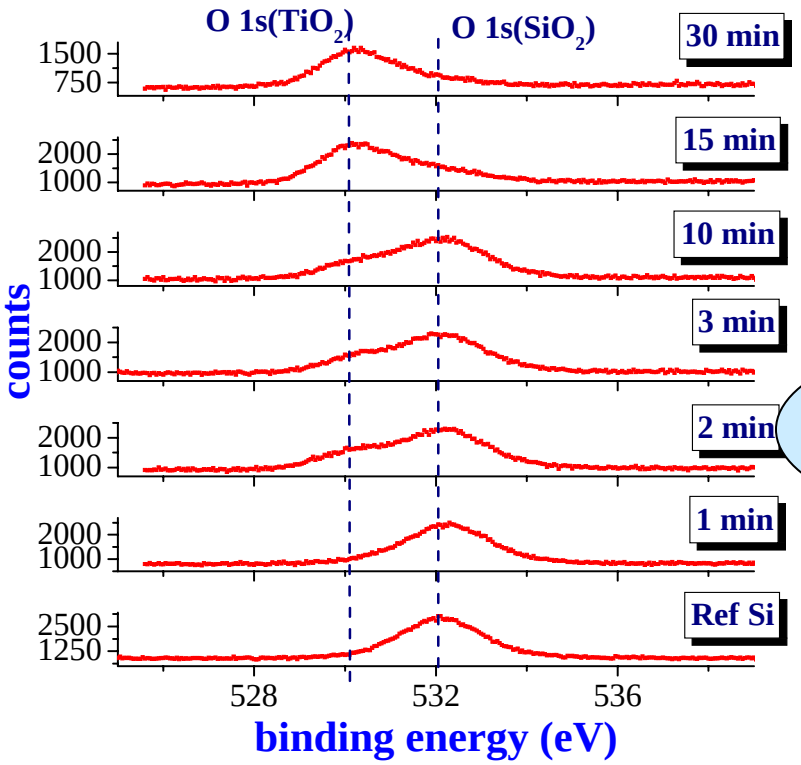

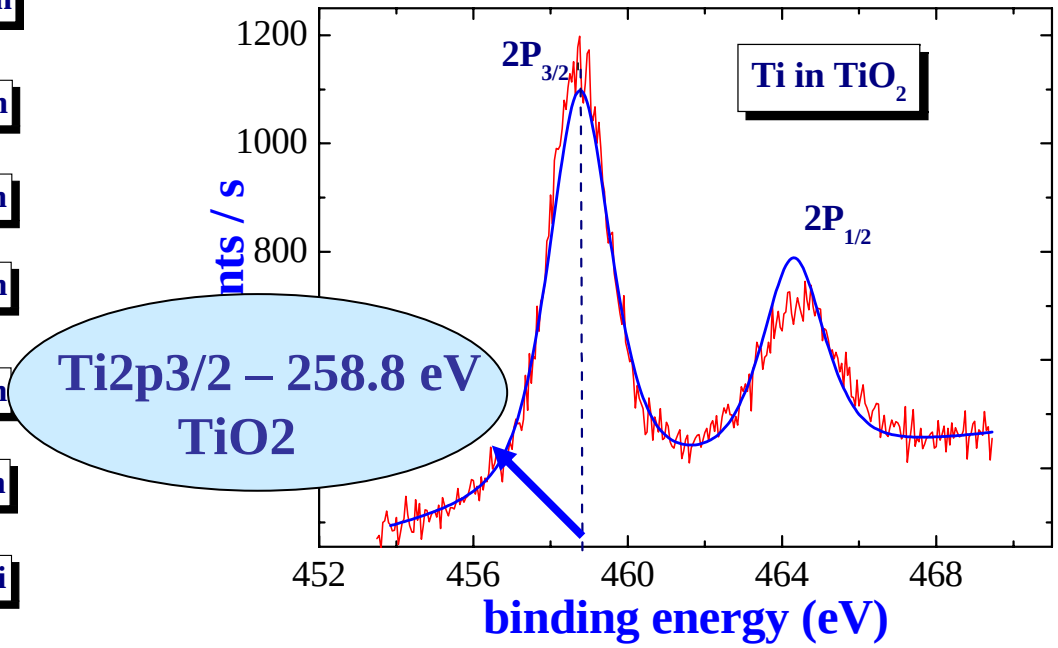

- Clusters on the surface are fully oxidised TiO_2

Size of deposited Ti cluster size

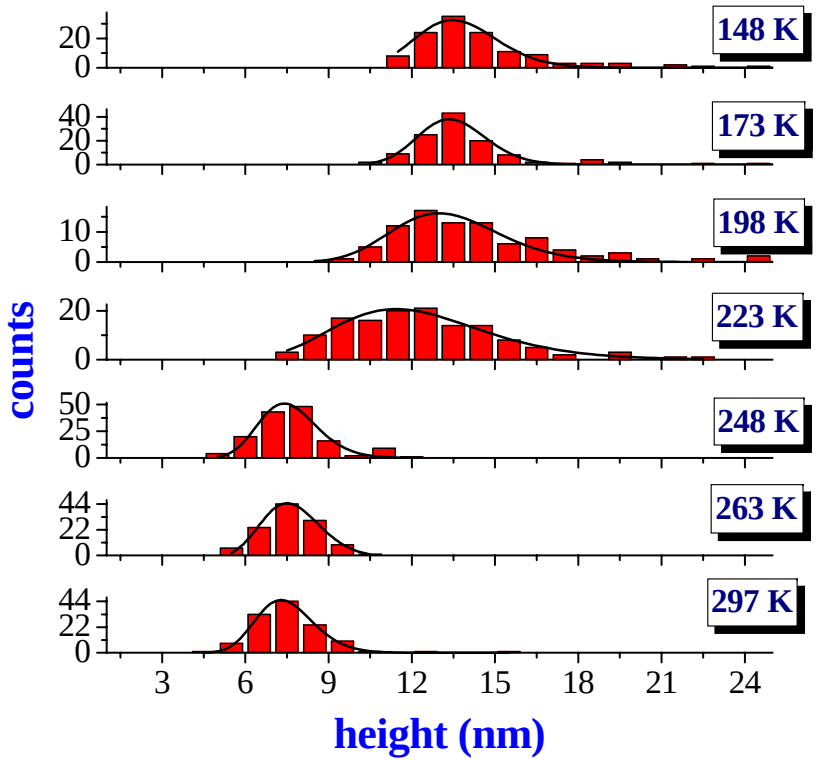

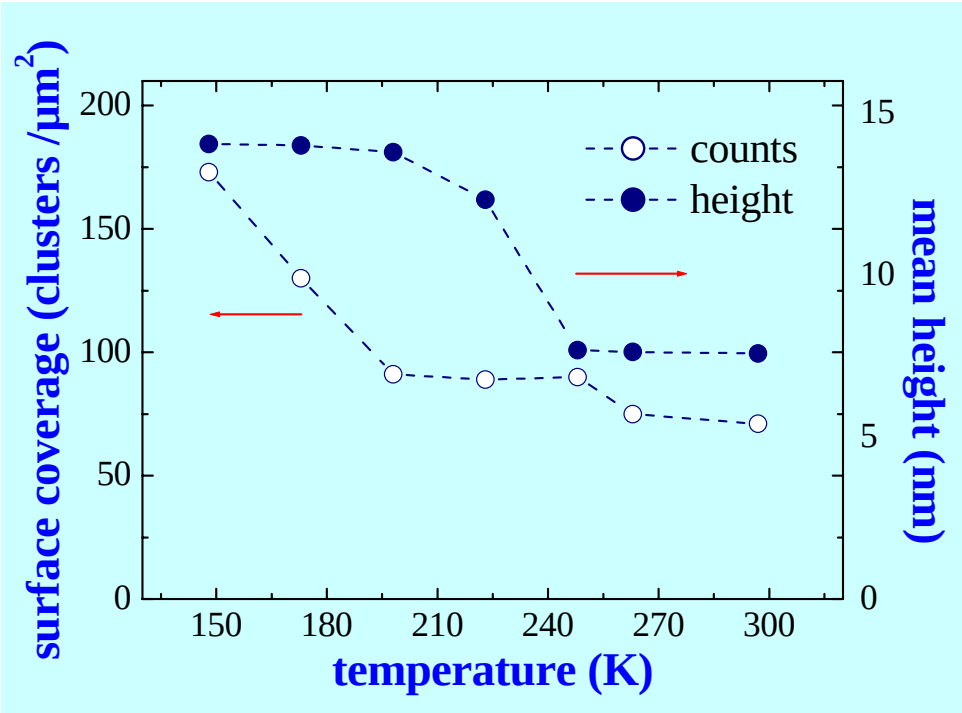

- the temperature dependence of size is due to the cluster-wall interaction

Deposition time 8 min

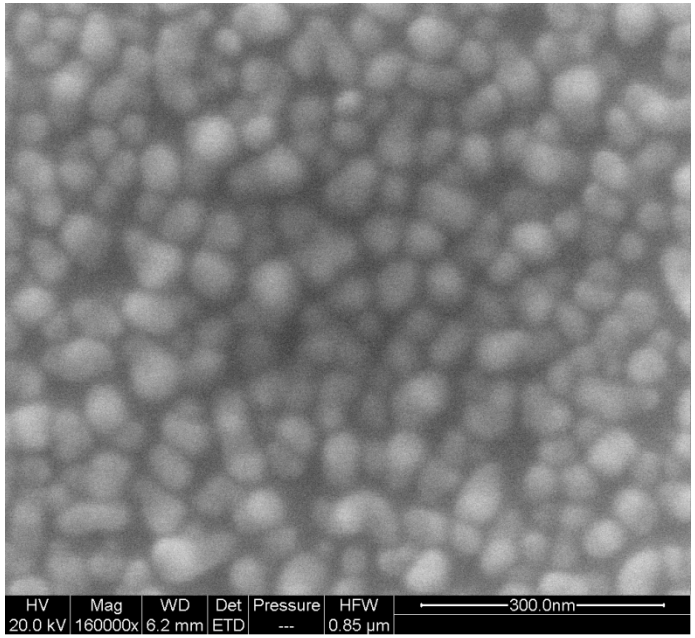

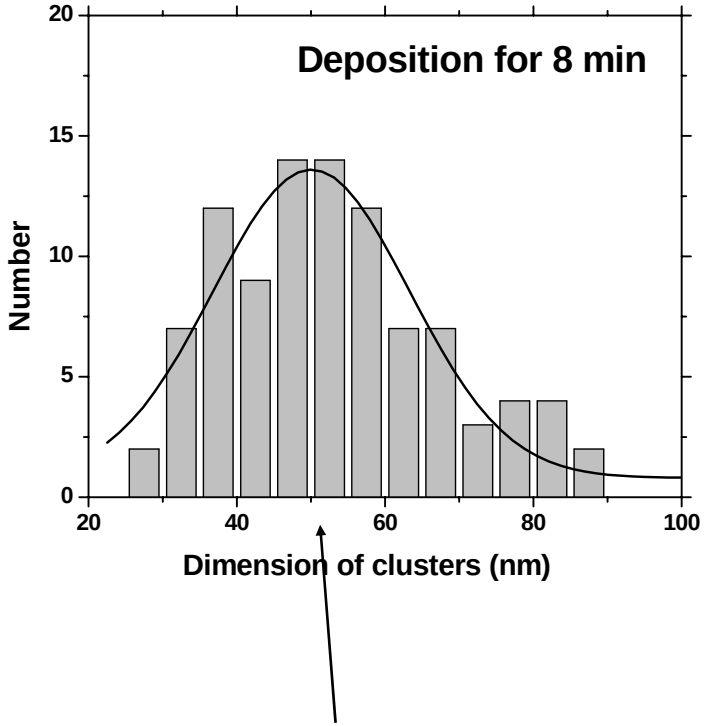

Clusters continue to grow on surfaces at prolonged depostion times

Mean size: 50 nm

Deposition time 15 min

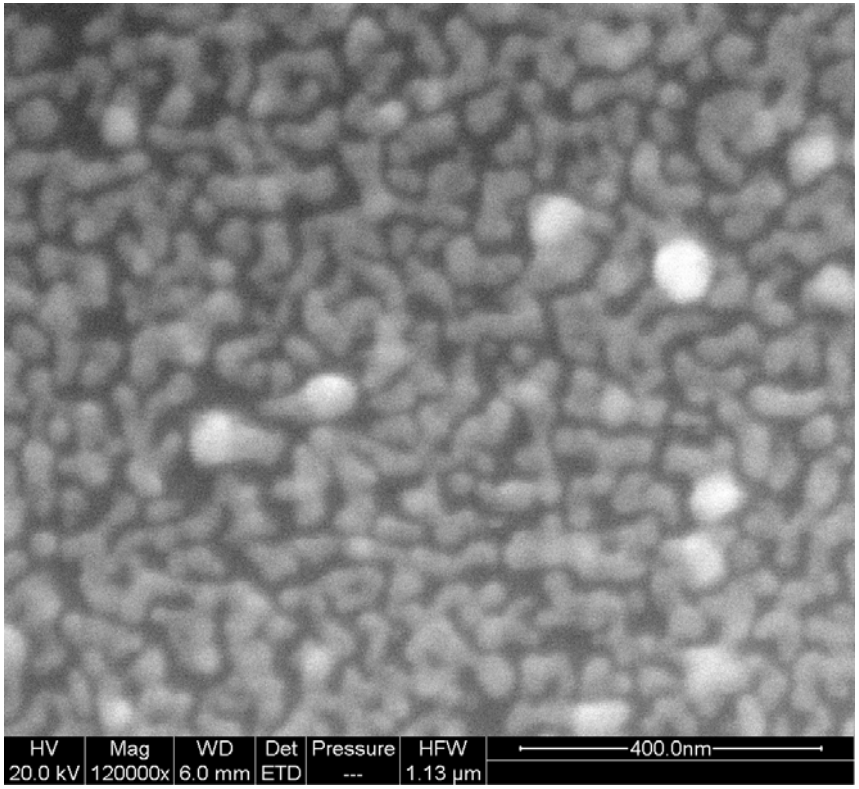

Deposited films from 5 nm clusters

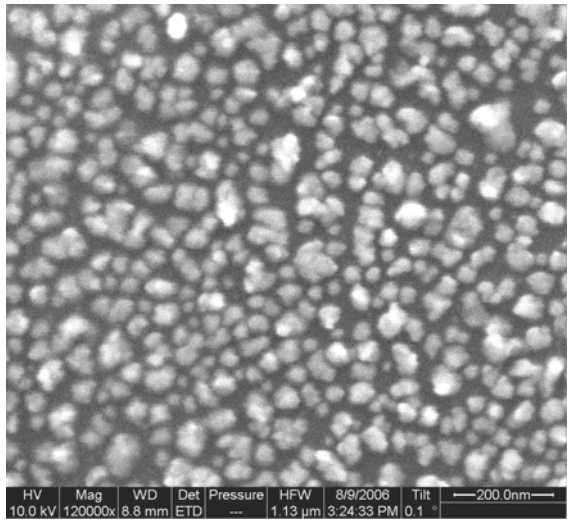

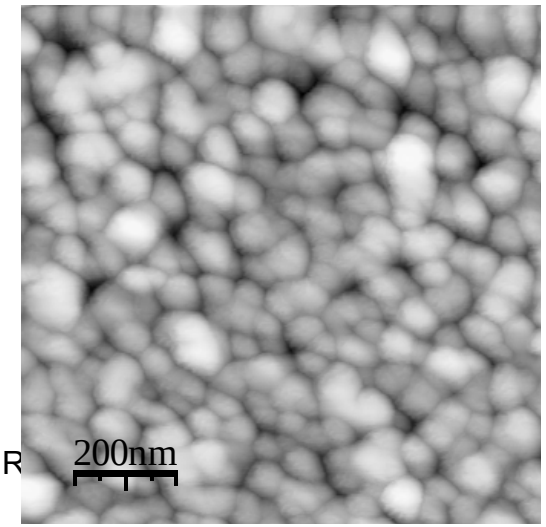

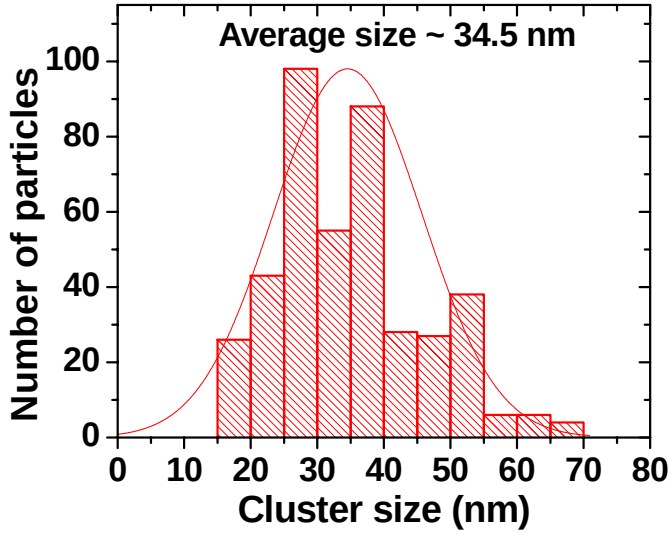

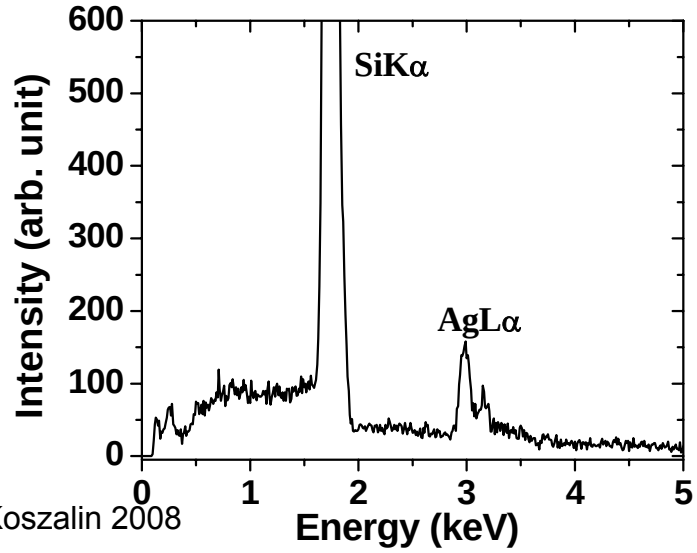

Rapid thermal annealing (473 K – 1073 K)

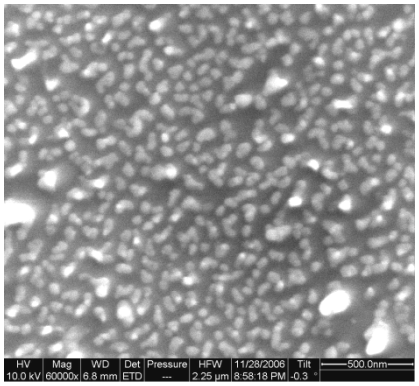

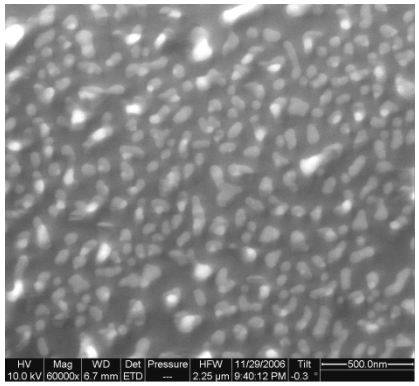

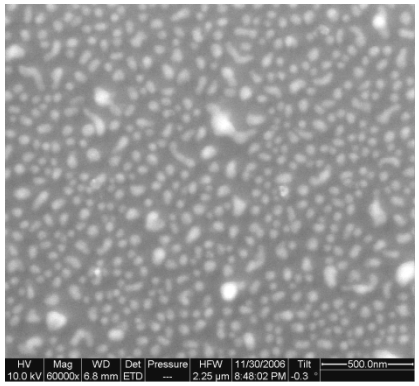

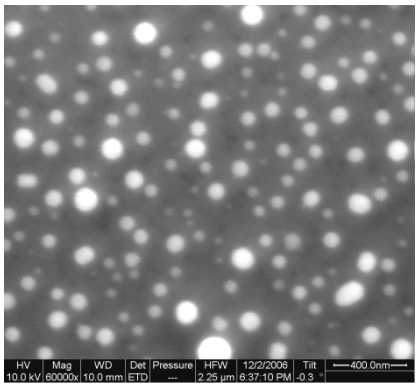

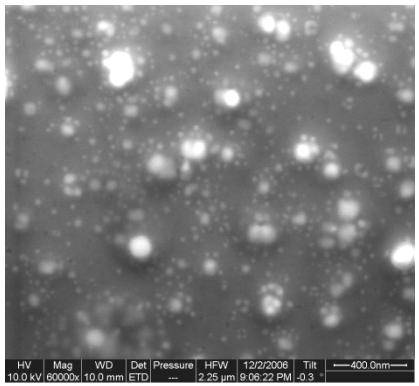

Rapid thermal annealing (873 K and 1073 K)

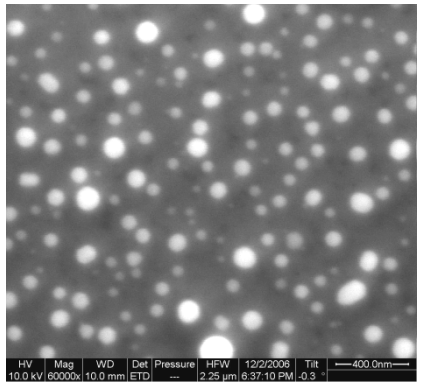

Mean size:
70 nm

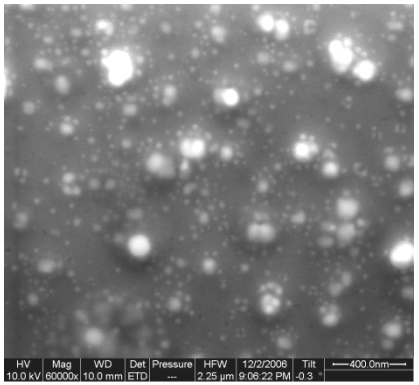

Two-sizes:
30 nm and
60 nm

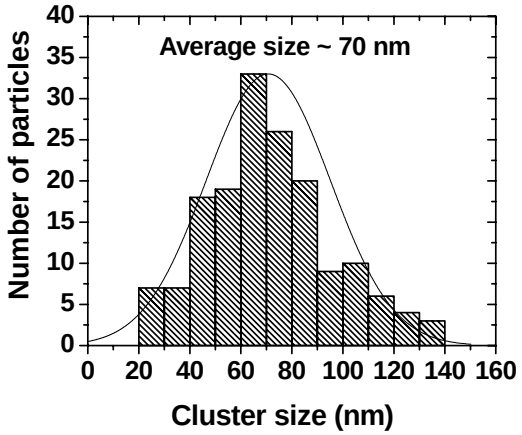

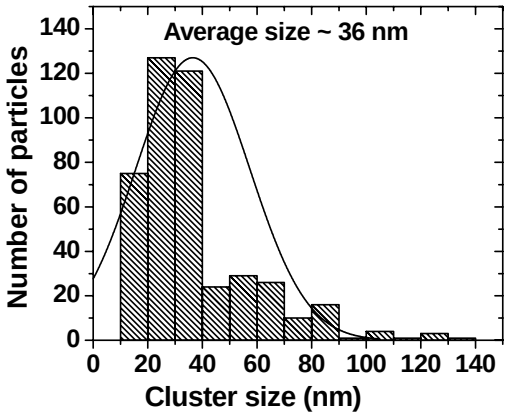

Fragmentation of nano-size clusters ?

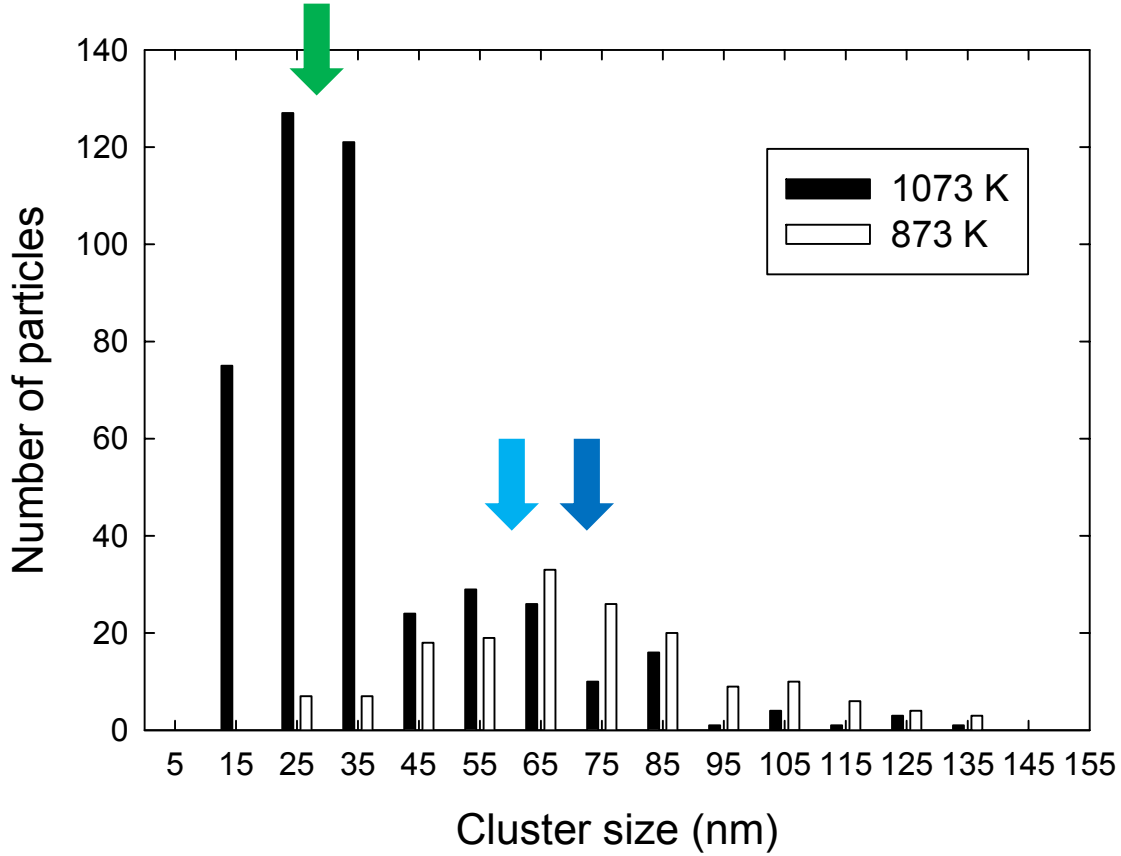

Fragmentation:

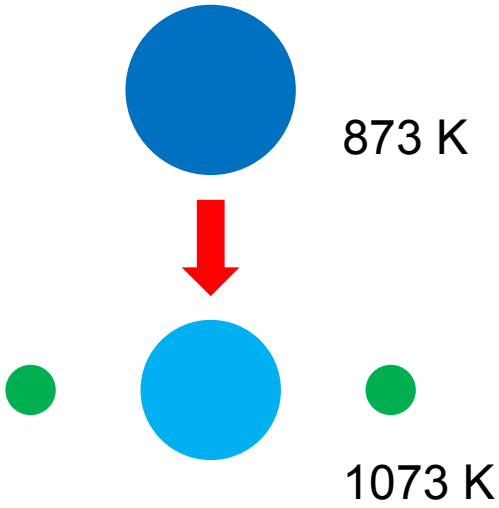

Conclusion

- Nano-size cluster show many interesting feature
- Much more work yet to be done

Thank you